J. Math. Computer Sci., 35 (2024), 182–207

Online: ISSN 2008-949X

Journal of Mathematics and Computer Science

Journal Homepage: www.isr-publications.com/jmcs

Optimal control of a multiple delay model for hepatitis B virus infection of hepatocytes with DNA-containing capsids, immune response and drug therapy

Check for updates

Pensiri Yosyingyong[a], Ratchada Viriyapong[a,*], Elvin J. Moore[b]

[a]*Department of Mathematics, Faculty of Science, Naresuan University, Phitsanulok, 65000, Thailand.*

[b]*Department of Mathematics, Faculty of Applied Science, King Mongkut's University of Technology North Bangkok, Bangkok, 10800, Thailand.*

Abstract

Since the number of patients with chronic hepatitis B virus (HBV) infection is still high globally, appropriate strategies for therapy control are required. In this study, we propose an HBV model consisting of six populations, namely uninfected hepatocytes, infected hepatocytes, HBV DNA-containing-capsids, free viruses, antibodies and cytotoxic T-lymphocytes. The model also includes an adaptive immune response, cure rate of infected hepatocytes, two time delays and two control therapies. The two time delays are delay of virus production after infection by HBV and delay of antigenic stimulation generating cytotoxic T-lymphocytes. The two optimal controls are a therapy for blocking new infection and a therapy for inhibiting viral production. The existence, uniqueness, non-negativity and boundedness of model solutions are first proved. The model is shown to have three equilibrium states, namely infection-free, immune-free and endemic. The basic reproduction number for the stability of the infection-free equilibrium is derived and a sensitivity analysis is carried out to determine the most important parameters to change to control the disease. Then optimal control and the Pontryagin maximum principle are used to maximize the concentrations of uninfected hepatocytes, antibodies and cytotoxic T-lymphocytes at minimum cost.

Keywords: Delay model, drug therapy, HBV-DNA containing capsids, hepatitis B virus, immune response, cytotoxic T-lymphocyte (CTLs), Pontryagin maximum principle.

2020 MSC: 00A71, 34A34, 49J15.

©2024 All rights reserved.

1. Introduction

Hepatitis B virus (HBV) is a virus of the hepatocytes in the liver. The virus can cause both acute and chronic disease, where chronic hepatitis B increases the risk of developing liver failure, liver cancer or cirrhosis. According to a report by the World Health Organization (WHO) in 2019 [60], there are approximately 1.5 million new HBV infections each year and 296 million people living with chronic hepatitis B infection. Despite the availability of vaccines and the use of antiviral therapy, HBV chronic infection remains a global health concern.

The therapy for HBV infection currently includes antiviral agents which can reduce viral replication and act as immunomodulators ([26, 27, 65]). These agents can reduce incidence of liver cancer, slow

*Corresponding author

Email addresses: pensiriy61@nu.ac.th (Pensiri Yosyingyong), ratchadapa@nu.ac.th (Ratchada Viriyapong), elvin.j@sci.kmutnb.ac.th (Elvin J. Moore)

doi: 10.22436/jmcs.035.02.05

Received: 2023-09-25 *Revised:* 2023-10-23 *Accepted:* 2024-03-29

cirrhosis progression and improve long term survival. However, as stated in the WHO report in 2019 [60], the therapy does not lead to cure and most people who start therapy must continue it for the rest of their lives.

When HBV infects the hepatocytes, the adaptive immunity plays a crucial role in the clearance of HBV infections, i.e., the cytotoxic T-lymphocyte (CTL) cells act to clear the HBV-infected hepatocytes via both cytolytic and noncytolytic mechanisms, leading to a reduction in levels of circulating virus ([14, 49, 58]). In addition, the antibodies which are produced by the B-cells neutralize free viral particles and prevent reinfection ([2, 58]). Further, during the infection, the infected hepatocytes will release the HBV DNA-containing capsids as mature virions which form after the virus is enveloped by both cellular membrane lipids and viral envelope proteins ([9, 17, 23]).

Mathematical models have been widely used to study and understand HBV infection. Some models include HBV treatment through drug therapy, e.g., the work of Lewin et al. [43] and Yosyingyong and Viriyapong [62], whereas some models include an adaptive immune response, e.g., the work of Yousfi et al. [64], Chenari et al. [13] and Manna et al. [49]. Further, some researchers have also included HBV DNA-containing capsids in their models, e.g., the papers by Manna et al. [46–49] and Harroudi et al. [28]. In addition, some researchers have included time delays in their model. For example, Gourley et al. [25] and Eikenberry et al. [19] have developed models including an explicit time delay in virus production, Farah et al. [20] have developed a time-delayed two-strain epidemic model with general incidence rates, Yosyingyong and Viriyapong [63] have studied the global dynamics of a within-host, multiple delay model for HBV infection which includes immune response and drug therapy, Manna et al. [49] have studied a generalized distributed delay model with two modes of transmission and adaptive immunity and Xu et al. [61] have studied global stability and bifurcation in a model with nonlinear incidence and multiple delays.

Optimal control theory has also been used to design control strategies for reduction of disease transmission or infection including HBV infection. Some examples of optimal control of delayed HBV infection models include the following. In 2016, Forde et al. [22] proposed a model which included immune effector cells and a time delay that accounted for the lag between the antigen encounter and the effector cell expansion. In 2017, Meskef et al. [51] developed a model that included an adaptive immune response with CTLs and antibodies and a time delay for virus production in the infected cells after viral entry. In 2017, Sun and Liu [57] proposed a new time delay HBV model with an incubation period and time delay for both virus production and immune response after viral entry into healthy cells. Sun and Liu also added a time delay into a drug therapy term which represented the effect of the drugs in reducing the infection rate from free viruses. In 2018, Allali et al. [3] further improved the model of Meskef et al. [51] by modifying the growth term of both healthy and infected hepatocyte cells to be logistic growth. In 2018, Danane et al. [17] proposed a new optimal control delay model which included HBV DNA-containing capsids and a single time delay with the same meaning as in the above models. This model was further improved by Danane et al. [16] who added antibodies into the model. In 2019, Meskef [50] further extended the work of Danane and Allali [16] by considering the fact that during therapy a fraction of infected hepatocytes could be cured and could revert back to healthy hepatocytes. In 2020, Khatun and Biswas [38] developed optimal control strategies for preventing HBV infection and reducing chronic liver cirrhosis incidence.

In the HBV infection models discused above, all optimal control time delay models for HBV infection have included only a single time delay. To the authors' knowledge, there is no optimal control model of multiple delays for HBV infection in the literature. In this study, we propose an optimal control model for drug therapy of HBV infection by considering two time delays, namely a virus production delay and an antigenic stimulation generating CTLs delay. The two controls in the model are drug therapy in blocking new infection and drug therapy in inhibiting viral production. In addition, we include HBV DNA-containing capsids and an adaptive immune response.

The paper is organized as follows. In Section 2, the model is introduced and the existence, uniqueness, non-negativity and boundedness of the solutions are proved. In Section 2, the properties of the equilibrium states are derived, including the basic reproduction number R_0, the local and global stability, and

the sensitivites of R_0 to changes in values of parameters. In Section 3, the optimal control theory of the model is presented and the existence of an optimal control pair is verified by the Pontryagin maximum principle. In Section 4, numerical simulations are presented and the results are discussed. Finally, Section 5 contains the conclusions.

2. Model formulation

The model we consider is an extension of the model of Meskef [50].

2.1. Definition of model

The model consists of six variables, namely the concentrations (units: mm^{-3}) of uninfected hepatocytes $x(t)$, infected hepatocytes $y(t)$, intracellular HBV DNA-containing capsids $c(t)$, free viruses $v(t)$, antibodies $w(t)$, and cytotoxic T-lymphocytes $z(t)$. The model also includes two time delays, namely a virus production delay τ_1 and an antigenic stimulation generating CTLs delay τ_2. In addition, we include two controls, namely a control $u_1(t)$ on the effectiveness of drug therapy in reducing new infections of hepatocytes, and a control $u_2(t)$ on the effectiveness of drug therapy in inhibiting viral production.

The equations for the model are shown in Eq. (2.1), the initial conditions are given in Eq. (2.2), and a flow chart for the model is shown in Fig. 1. The definitions and assumed values for all parameters are shown in Table 1,

$$\begin{aligned}
\frac{dx}{dt} &= \Lambda - \sigma x(t) - (1-u_1(t))\beta x(t)v(t) + py(t),\\
\frac{dy}{dt} &= (1-u_1(t))\beta e^{-m\tau_1}x(t-\tau_1)v(t-\tau_1) - (\sigma+p)y(t) - qy(t)z(t),\\
\frac{dc}{dt} &= (1-u_2(t))ay(t) - \alpha c(t) - \delta c(t),\\
\frac{dv}{dt} &= \alpha c(t) - \gamma v(t)w(t) - \mu v(t),\\
\frac{dw}{dt} &= gv(t)w(t) - hw(t),\\
\frac{dz}{dt} &= ky(t-\tau_2)z(t-\tau_2) - \varepsilon z(t),
\end{aligned} \tag{2.1}$$

where $\{x(t), y(t), c(t), v(t), w(t), z(t)\} \in \Re^6$ are state variables, $\tau_1 > 0$ and $\tau_2 > 0$ are time delays, and $u_1(t) \in [0,1]$, $u_2(t) \in [0,1]$ are control variables. Then, for the maximum time delay $\tau = \max\{\tau_1, \tau_2\}$ and for nonnegative constants $x_0, y_0, c_0, v_0, w_0, z_0$, we define the initial conditions for the system of state equations (2.1) as follows. For $t \in [-\tau, 0]$, let

$$x(t) = x_0 \geqslant 0,\ y(t) = y_0 \geqslant 0,\ c(t) = c_0 \geqslant 0,\ v(0) = v_0 \geqslant 0,\ w(t) = w_0 \geqslant 0,\ z(t) = z_0 \geqslant 0. \tag{2.2}$$

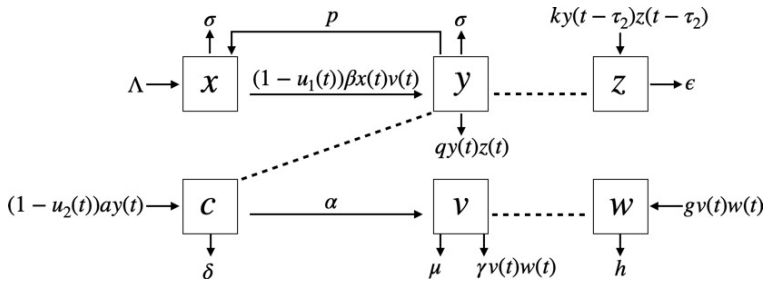

Figure 1: The flow chart of the delay model of HBV infection including immune response and optimal control of drug therapy. The solid lines represent the transferring from one class to another class, whereas the dotted lines represent an involvement or influence of one class on another class.

Table 1: Definitions and sources of values of parameters used in the model (2.1).

Parameter	Meaning	Value	Units	Source
$u_1(t)$	Efficiency of drug therapy in blocking new infection	0–1	fraction	-
$u_2(t)$	Efficiency of drug therapy in inhibiting viral production	0–1	fraction	-
Λ	Production rate of uninfected hepatocytes	1	$day^{-1}mm^{-3}$	[32]
σ	Natural death rate of hepatocytes.	0.011	day^{-1}	[25]
β	Rate of infection of hepatocytes by the free virus	0.0014	mm^3day^{-1}	[32]
$e^{-m\tau_1}$	Probability of surviving of hepatocytes in the time period from $t-\tau_1$ to t			
m	Death rate of infected hepatocytes in the time period from $t-\tau_1$ to t	0.011	day^{-1}	[51]
τ_1	Delay in the production of infected hepatocytes.	2	day	assumed
τ_2	Delay in antigenic stimulation generating CTLs.	4	day	assumed
p	Cure rate of infected hepatocytes by non-cytolytic cure process.	0.01, 0.012	day^{-1}	[66]
q	Death rate of infected hepatocytes due to the CTLs response.	0.001	mm^3day^{-1}	[17]
a	Production rate of intracellular HBV DNA-containing capsids.	0.15	day^{-1}	assumed
α	Growth rate of virions in blood.	0.87	day^{-1}	[15]
δ	Clearance rate of intracellular HBV DNA-containing capsids.	0.053	day^{-1}	[47]
γ	Rate that viruses are neutralized by antibodies.	0.01	mm^3day^{-1}	[51]
μ	Death rate of free viruses.	0.0693	day^{-1}	[32]
g	Expansion rate of antibodies in response to free viruses.	0.008	mm^3day^{-1}	[15]
h	Decay rate of antibodies.	0.15	day^{-1}	[51]
k	Expansion rate of CTLs in response to viral antigen derived from infected hepatocytes.	0.001	mm^3day^{-1}	assumed
ε	Decay rate of CTLs in the absence of antigenic stimulation.	0.5	day^{-1}	[1]

Note that, in Table 1, we assumed values for parameters τ_1, τ_2, a, and k. Our motivation for the value for τ_1 comes from the works by Meskaf et al. [51], Danane et al. [17], and Manna [45], who used values for τ_1 ranging from 0.5 to 5; therefore we assumed the value 2. Zhuang [67] and Sun and Liu [57] used values ranging from 0.03 to 10 for τ_2; we assumed a value equal to 2. Next, in Manna and Hattaf [48] a production rate of intracellular HBV DNA-containing capsids (a in our model) was taken to be 1.5, while the production rate of uninfected cells (Λ in our model) was 10. In our study Λ equals 1, and we set a equal to 0.15. Finally, the expansion rate of CTLs in response to viral antigen derived from infected hepatocytes (k in our model) equals 0.0012 in the work of Harroudi et al. [28]; we assumed this value to be 0.001.

2.2. *Nonnegativity and boundedness of solutions*

In this paper, we are interested in finding optimal conditions on the control variables $u_1(t)$ and $u_2(t)$ that drive the infected hepacyte population $y(t)$ or the free virus population $v(t)$ to zero. Therefore, starting with the nonnegative initial conditions (2.2), we will integrate the system up to a finite time T

defined as in Theorem 2.1.

We now prove the following theorem.

Theorem 2.1. *Solutions of system (2.1) with initial conditions (2.2) are nonnegative for $-\tau \leqslant t \leqslant T$, where $T = \min\{T_f, T_y, T_v\}$ where T_f is a specified finite time, T_y is the time at which $y(t)$ first becomes zero and T_v is the time at which the population of free viruses $v(t)$ first becomes zero.*

Proof. As stated in (2.2), the initial values of the variables of system (2.1) are assumed to be nonnegative for $t \in [-\tau, 0]$. We now prove that all variables are nonnegative for $0 \leqslant t \leqslant T$.

We first note that the variables $y(t)$ and $v(t)$ cannot become negative for $0 < t \leqslant T$ since, by definition of T, $y(t) \geqslant 0$ for $0 \leqslant t = T_y \geqslant T$ and $v(t) \geqslant 0$ for $0 \leqslant t = T_v \geqslant T$. We now look at possible solutions of the equations in (2.1). We begin with the x equation:

$$\frac{dx}{dt} = \Lambda - (\sigma - (1 - u_1(t))\beta v(t))x(t) + py(t).$$

In this case, if $y(t) = 0$, the equation becomes

$$\frac{dx_1}{dt} = \Lambda - (\sigma - (1 - u_1(t))\beta v(t))x_1(t),$$

and the solution is $x_1(t) = \Lambda t + x_1(0)e^{-\int_0^t (1-u_1(s))\beta v(s)\,ds} > 0$, since $\Lambda > 0$ and $x_1(0) \geqslant 0$. Next, since $y(t) > 0$ for $t < T$ and $y(T) \geqslant 0$, we have $\frac{dx}{dt} > \frac{dx_1}{dt}$ for $t < T$ and $\frac{dx}{dt} \geqslant \frac{dx_1}{dt}$ for $t = T$, and therefore $x(t) \geqslant x_1(t) > 0$ for $t \leqslant T$. The c equation is

$$\frac{dc}{dt} = (1 - u_2(t))\alpha y(t) - (\alpha + \delta)c(t).$$

If $y(t) = 0$, then the equation becomes $\frac{dc_1}{dt} = -(\alpha + \delta)c_1(t)$ and the solution is $c_1(0)e^{-(\alpha+\delta)t} > 0$ since $c_1(0) \geqslant 0$. Next, since $y(t) > 0$ for $t < T$ and $y(T) \geqslant 0$, we have $\frac{dc}{dt} > \frac{dc_1}{dt}$ for $t < T$ and $\frac{dc}{dt} \geqslant \frac{dc_1}{dt}$ for $t = T$, and therefore $c(t) \geqslant c_1(t) > 0$ for $t \leqslant T$. The w equation is

$$\frac{dw}{dt} = (gv(t) - h)w(t),$$

which has the exponential solution $w(t) = w(0)e^{\int_0^t (gv(s)-h)\,ds}$. Since, by assumption, $w(0) \geqslant 0$, we have $w(t) \geqslant 0$ for all $t > 0$. The z equation is

$$\frac{dz}{dt} = ky(t - \tau_2)z(t - \tau_2) - \varepsilon z(t).$$

We first note that the equation $\dot{z}_1(t) = -\varepsilon z_1(t)$ has the solution $z_1(t) = z_1(0)e^{-\varepsilon t} \geqslant 0$ for all $t \geqslant 0$ if $z_1(0) \geqslant 0$. Also, we have $y(t - \tau_2) > 0$ for $0 \leqslant t \leqslant T + \tau_2$. Hence, if $z(t - \tau_2) \geqslant 0$ for $0 \leqslant t \leqslant T + \tau_2$, we have $\dot{z}(t) \geqslant \dot{z}_1(t)$ and $z(t) \geqslant z_1(t) > 0$. Note that, in this case, since $z(t) \geqslant 0$ for $-\tau_2 \leqslant t \leqslant 0$, we have that $z(t)$ cannot become zero, unless $z(t - \tau_2)$ is already negative. The proof is complete. □

We will next prove that the solutions are bounded above.

Theorem 2.2. *For each solution $X(t)$ of an equation in system (2.1) there exists an upper bound (supremum $\overline{X}$) such that if $0 \leqslant X(t) \leqslant \overline{X}$ for $t \in [-\tau, 0]$, then $X(t) \leqslant \overline{X}$ for all $0 < t \leqslant T$.*

Proof. We have already proved in Theorem 2.1 that all variables are nonnegative for all $0 \leqslant t \leqslant T$, and therefore they are bounded below. In the proof, we will use the following Condition 1.

Condition 1: If a variable $X(t)$ and derivative $\frac{dX}{dt}$ are continuous, a necessary and sufficient condition for the solution $X(t)$ of a differential equation variable to be bounded above (i.e., for a supremum $\overline{X}$ to exist) is that $X(0) \leqslant \overline{X}$ and that $\frac{dX}{dt} \leqslant 0$ for $X(t) \geqslant \overline{X}$ for all $0 \leqslant t \leqslant T$.

Note that, in this definition, we are assuming that it is possible to substitute initial conditions in the differential equation that give a solution greater than or equal to the supremum, but the derivative must then be negative or zero for all such initial conditions.

We will use Condition 1 to prove that all variables in the system (2.1) are bounded above for $0 \leqslant t \leqslant T$. Without loss of generality, we will assume that $x(t) + y(t) \leqslant \frac{\Lambda}{\sigma}$ for $t \in [-\tau, 0]$. We will first consider the variables x and y in system (2.1). From x and y equations in system (2.1), we have

$$\frac{d(x+y)}{dt} = \Lambda - \sigma(x(t)+y(t)) - qy(t)z(t) - (1-u_1(t))\beta\left(x(t)v(t) - e^{-m\tau_1}x(t-\tau_1)v(t-\tau_1)\right). \tag{2.3}$$

Clearly, from (2.3), if

$$x(t)v(t) - e^{-m\tau_1}x(t-\tau_1)v(t-\tau_1) \geqslant 0, \tag{2.4}$$

then, since $y \geqslant 0$ and $z \geqslant 0$, we have $\frac{d(x+y)}{dt} \leqslant 0$ for $x + y \geqslant \frac{\Lambda}{\sigma}$, and therefore $x + y \leqslant \frac{\Lambda}{\sigma}$ is bounded above. Also, since x and y are nonnegative, both x and y must be bounded above. However, in this case, it is possible that $v(t)$ is unbounded.

On the other hand, if condition (2.4) is not satisfied, then it is possible that $\frac{d(x+y)}{dt} > 0$ for all $x + y$ and that $x + y$ is not bounded. However, this case can only occur if $x(t)v(t)$ is a decreasing function of t in which case $x(t)v(t)$ must be bounded. In this case, it is possible that $y(t)$ could be unbounded.

The possibilities from (2.3) are therefore as follows.

Case 1. x and v are bounded and y is unbounded.

Case 2. x and y are bounded and v is unbounded.

Case 3. x, v, and y are all bounded.

We next prove that Case 1 is impossible, i.e., we prove that if x and v are bounded, then y is also bounded. Let $\bar{x}$ and $\bar{v}$ be the upper bounds on x and v, respectively. Then, from y equation in (2.1), we have

$$\begin{aligned}\frac{dy}{dt} &= (1-u_1(t))\beta e^{-m\tau_1}x(t-\tau_1)v(t-\tau_1) - (\sigma+p)y(t) - qy(t)z(t)\\ &\leqslant (1-u_1(t))\beta e^{-m\tau_1}\bar{x}\bar{v} - (\sigma+p)y(t) - qy(t)z(t) \leqslant 0 \ \text{ for } \ y(t) \geqslant \frac{(1-u_1(t))\beta e^{-m\tau_1}\bar{x}\bar{v}}{\sigma+p}.\end{aligned}$$

Therefore, using Condition 1, we have $y(t)$ is bounded above by $\bar{y} = \frac{(1-u_1(t))\beta e^{-m\tau_1}\bar{x}\bar{v}}{(\sigma+p)}$.

Hence, the only two possibilities are Cases 2 and 3, i.e., that x and y are bounded above and v is either bounded or unbounded. We now consider the equations for $\frac{dc}{dt}$, $\frac{dv}{dt}$, $\frac{dw}{dt}$, and $\frac{dz}{dt}$ in (2.1). We assume that $\bar{x}$ and $\bar{y}$ are the upper bounds on x and y, respectively. In the proofs, we use Condition 1 to prove that each variable is bounded above.

1. For $c(t)$, we have from (2.1) that

$$\frac{dc}{dt} = (1-u_2(t))ay(t) - \alpha c(t) - \delta c(t) \leqslant (1-u_2(t))a\bar{y} - (\alpha+\delta)c(t) \leqslant 0 \ \text{ for } \ c(t) \geqslant \frac{(1-u_2(t))a\bar{y}}{\alpha+\delta}.$$

Therefore, $c(t)$ is bounded above by $\bar{c} = \frac{(1-u_2(t))a\bar{y}}{\alpha+\delta}$.

For $v(t)$, we have

$$\frac{dv}{dt} = \alpha c(t) - \gamma v(t)w(t) - \mu v(t) \leqslant \alpha\bar{c} - (\gamma w(t)+\mu)v(t) \leqslant 0 \ \text{ for } \ v(t) \geqslant \frac{\alpha\bar{c}}{\gamma w(t)+\mu}.$$

Therefore, since $w \geqslant 0$, $v(t)$ is bounded above by $\bar{v} = \frac{\alpha\bar{c}}{\mu}$. We have therefore proved that Case 3 above is the only possibility.

2. For $w(t)$, we have

$$\frac{dw}{dt} = gv(t)w(t) - hw(t) \leqslant (g\bar{v} - h)w(t).$$

For the model that we are considering it is clear that the extra condition $h > g\bar{v}$ is required to prove boundedness of the antibody concentration w.

3. For $z(t)$, we have

$$\frac{dz}{dt} = ky(t-\tau_2)z(t-\tau_2) - \varepsilon z(t) \leqslant (k\bar{y} - \varepsilon)z(t).$$

For the model that we are considering it is clear that the extra condition $\varepsilon > k\bar{y}$ is required to prove boundedness of the concentration of cytotoxic T-lymphocytes $z(t)$. The proof is complete. □

2.3. Existence of unique solution

Theorem 2.3. *System (2.1) with specified initial conditions (2.2) and specified values of the controls $(u_1(t), u_2(t))$ has a unique solution.*

Proof. We will prove that the system (2.1) satisfies Lipschitz conditions (see, e.g., [8, 18]) and therefore that the solution exists and is unique.

Note that, in the proof, we are assuming that the control functions $(u_1(t), u_2(t))$ are fixed functions and that $u_1(t) \in [0,1]$ and $u_2(t) \in [0,1]$. Changing the values of these functions will, of course, change the solution.

Following Driver [18] (section V-23), we rewrite system (2.1) in the form

$$\frac{dX}{dt} = F(t, \xi_t), \quad X(t) \text{ given, } t \in [-\tau, 0], \tag{2.5}$$

where, as above, $\tau = \max\{\tau_1, \tau_2\}$, and where we define

$$X(t) = \begin{bmatrix} x(t) \\ y(t) \\ c(t) \\ v(t) \\ w(t) \\ z(t) \end{bmatrix}, \qquad \xi_t = \left[\xi_{1,t}, \xi_{2,t}\right] = \begin{bmatrix} x(t) & x(t-\tau_1) \\ y(t) & y(t-\tau_2) \\ c(t) & 0 \\ v(t) & v(t-\tau_1) \\ w(t) & 0 \\ z(t) & z(t-\tau_2) \end{bmatrix}, \tag{2.6}$$

and

$$\begin{aligned}
F_1(t, \xi_t) &= \Lambda - \sigma x(t) - (1-u_1(t))\beta x(t)v(t) + py(t), \\
F_2(t, \xi_t) &= (1-u_1(t))\beta e^{-m\tau_1} x(t-\tau_1)v(t-\tau_1) - (\sigma + p)y(t) - qy(t)z(t), \\
F_3(t, \xi_t) &= (1-u_2(t))ay(t) - \alpha c(t) - \delta c(t), \\
F_4(t, \xi_t) &= \alpha c(t) - \gamma v(t)w(t) - \mu v(t), \\
F_5(t, \xi_t) &= gv(t)w(t) - hw(t), \\
F_6(t, \xi_t) &= ky(t-\tau_2)z(t-\tau_2) - \varepsilon z(t).
\end{aligned} \tag{2.7}$$

We now prove that the system (2.5)-(2.7) satisfies the Lipschitz condition of Driver [18] (Definition Eq. (4), p.258), i.e.,

$$\|F(t, \xi_t) - F(t, \hat{\xi}_t)\|_1 \leqslant L\|\xi_t - \hat{\xi}_t\|_1, \tag{2.8}$$

for some $L > 0$ and where the one-norm $\|\xi_t - \hat{\xi}_t\|_1$ is the maximum absolute column sum of $\xi_t - \hat{\xi}_t$ (see, e.g., Anton [4]). We begin by writing system (2.5) in the following matrix form:

$$F(t, \xi_t) = A(t)\xi_{1,t} + B(\xi_{1,t}) + C(\xi_{2,t}),$$

where

$$A(t) = \begin{bmatrix} -\sigma & p & 0 & 0 & 0 & 0 \\ 0 & -(\sigma+p) & 0 & 0 & 0 & 0 \\ 0 & (1-u_2(t))a & -(\alpha+\delta) & 0 & 0 & 0 \\ 0 & 0 & \alpha & -\mu & 0 & 0 \\ 0 & 0 & 0 & 0 & -h & 0 \\ 0 & 0 & 0 & 0 & 0 & -\varepsilon \end{bmatrix},$$

$$B(\xi_{1,t}) = \begin{bmatrix} \Lambda - (1-u_1(t))\beta x(t)v(t) \\ -qy(t)z(t) \\ 0 \\ -\gamma v(t)w(t) \\ gv(t)w(t) \\ 0 \end{bmatrix},$$

$$C(\xi_{2,t}) = \begin{bmatrix} 0 \\ (1-u_1(t))\beta e^{-m\tau_1} x(t-\tau_1)v(t-\tau_1) \\ 0 \\ 0 \\ 0 \\ ky(t-\tau_2)z(t-\tau_2) \end{bmatrix}. \tag{2.9}$$

The next step is to prove that the function $F(t, \xi_t)$ satisfies the Lipschitz conditions in (2.8). We first note that, from the properties of norms,

$$\begin{aligned} \|F(t, \xi_t) - F(t, \hat{\xi}_t)\|_1 &= \|A(t)(\xi_1(t) - \hat{\xi}_{1,t}) + B(\xi_{1,t}) - B(\hat{\xi}_{1,t}) + C(\xi_{2,t}) - C(\hat{\xi}_{2,t})\|_1 \\ &\leqslant \|A(t)(\xi_{1,t} - \hat{\xi}_{1,t})\|_1 + \|B(\xi_{1,t}) - B(\hat{\xi}_{1,t})\|_1 + \|C(\xi_{2,t}) - C(\hat{\xi}_{2,t})\|_1. \end{aligned} \tag{2.10}$$

We consider each term in (2.10) separately. For the $A(t)$ term, we have

$$\|A(t)(\xi_{1,t} - \hat{\xi}_{1,t})\|_1 \leqslant \|A(t)\|_1 \|\xi_{1,t} - \hat{\xi}_{1,t}\|_1 = L_1(t)\|\xi_{1,t} - \hat{\xi}_{1,t}\|_1, \tag{2.11}$$

where $L_1(t) = \|A(t)\|_1 = \max\{\sigma,\ \sigma + 2p + (1-u_2(t))a,\ \alpha+\delta,\ \mu,\ h,\ \varepsilon\}$ is the maximum absolute column sum of $A(t)$.

For the one-norm of $B(\xi_{1,t}) - B(\hat{\xi}_{1,t})$, we have

$$\|B(\xi_{1,t}) - B(\hat{\xi}_{1,t})\|_1 = \left\| \begin{matrix} (-(1-u_1(t))\beta[x_1(t)v_1(t) - \hat{x}_1(t)\hat{v}_1(t)] \\ -q[y_1(t)z_1(t) - \hat{y}_1(t)\hat{z}_1(t)] \\ 0 \\ -\gamma[v_1(t)w_1(t) - \hat{v}_1(t)\hat{w}_1(t)] \\ g[v_1(t)w_1(t) - \hat{v}_1(t)\hat{w}_1(t))] \\ 0 \end{matrix} \right\|_1.$$

Then, since the one-norm of a vector is the sum of absolute values of components, and since the absolute value of a product of the form $x_1y_1 - \hat{x}_1\hat{y}_1$ can be rewritten as

$$\begin{aligned} |x_1(t)y_1(t) - \hat{x}_1(t)\hat{y}_1(t)| &= |[x_1(t) - \hat{x}_1(t)]y_1(t) + \hat{x}_1(t)[y_1(t) - \hat{y}_1(t)]| \\ &\leqslant |(x_1(t) - \hat{x}_1(t))||y_1(t)| + |\hat{x}_1(t)||(y_1(t) - \hat{y}_1(t)|, \end{aligned} \tag{2.12}$$

we can obtain the following:

$$\begin{aligned}
|B(\xi_{1,t}) - B(\hat{\xi}_{1,t})|_1 &= |(1-u_1(t))\beta[x_1(t)v_1(t) - \hat{x}_1(t)\hat{v}_1(t)]| + |q([y_1(t)z_1(t) - \hat{y}_1(t)\hat{z}_1(t)]| \\
&\quad + |\gamma[v_1(t)w_1(t) - \hat{v}_1(t)\hat{w}_1(t)]| + |g[v_1(t)w_1(t) - \hat{v}_1(t)\hat{w}_1(t)]| \\
&\leqslant (1-u_1(t))\beta|x_1(t) - \hat{x}_1(t)||v_1(t)| + (1-u_1(t))\beta|\hat{x}_1(t)||v_1(t) - \hat{v}_1(t)| \\
&\quad + q|y_1(t) - \hat{y}_1(t)||z_1(t)| + q|\hat{y}_1(t)||z_1(t) - \hat{z}_1(t)| \\
&\quad + (\gamma+g)|v_1(t) - \hat{v}_1(t)||w_1(t)| + (\gamma+g)|\hat{v}_1(t)||w_1(t) - \hat{w}_1(t)| \\
&= (1-u_1(t))\beta|v_1(t)||x_1(t) - \hat{x}_1(t)| + q|z_1(t)||y_1(t) - \hat{y}_1(t)| \\
&\quad + ((1-u_1(t))\beta|\hat{x}_1(t)| + (\gamma+g)|w_1(t)|)\,|v_1(t) - \hat{v}_1(t)| \\
&\quad + (\gamma+g)|\hat{v}_1(t)||w_1(t) - \hat{w}_1(t)| + q|\hat{y}_1(t)||z_1(t) - \hat{z}_1(t)|.
\end{aligned}$$

Then, defining $L_2(t)$ as

$$L_2(t) = \max\{(1-u_1(t))\beta|v_1(t)|,\ q|z_1(t)|, ((1-u_1(t))\beta|\hat{x}_1(t)| + (\gamma+g)|w_1(t)|)\,,\ (\gamma+g)|\hat{v}_1(t)|,\ q|\hat{y}_1(t)|\},$$

we obtain

$$\begin{aligned}
|B(\xi_{1,t}) - B(\hat{\xi}_{1,t})|_1 &\leqslant L_2(t)\,(|x_1(t) - \hat{x}_1(t)| + |y_1(t) - \hat{y}_1(t)| + |v_1(t) - \hat{v}_1(t)| \\
&\quad + |w_1(t) - \hat{w}_1(t)| + |z_1(t) - \hat{z}_1(t)|) \\
&\leqslant L_2(t)\,(|x_1(t) - \hat{x}_1(t)| + |y_1(t) - \hat{y}_1(t)| + |c_1(t) - \hat{c}_1(t)| \\
&\quad + |v_1(t) - \hat{v}_1(t)| + |w_1(t) - \hat{w}_1(t)| + |z_1(t) - \hat{z}_1(t)|) = L_2(t)\|\xi_{1,t} - \hat{\xi}_{1,t}\|_1.
\end{aligned} \tag{2.13}$$

For the one-norm $\|C(\xi_{2,t}) - C(\hat{\xi}_{2,t})\|_1$, we have from (2.9) and using (2.12) that

$$\begin{aligned}
\|C(\xi_{2,t}) - C(\hat{\xi}_{2,t})\|_1 &= (1-u_1(t))\beta e^{-m\tau_1}|x_1(t-\tau_1)v_1(t-\tau_1) - \hat{x}_1(t-\tau_1)\hat{v}_1(t-\tau_1)| \\
&\quad + k|y_1(t-\tau_2)z_1(t-\tau_2) - \hat{y}_1(t-\tau_2)\hat{z}_1(t-\tau_2)| \\
&\leqslant (1-u_1(t))\beta e^{-m\tau_1}|v_1(t-\tau_1)||x_1(t-\tau_1) - \hat{x}_1(t-\tau_1)| \\
&\quad + (1-u_1(t))\beta e^{-m\tau_1}|\hat{x}_1(t-\tau_1)||v_1(t-\tau_1) - \hat{v}_1(t-\tau_1)| \\
&\quad + k|z_1(t-\tau_2)||y_1(t-\tau_2) - \hat{y}_1(t-\tau_2)| + k|\hat{y}_1(t-\tau_2)||z_1(t-\tau_2) - \hat{z}_1(t-\tau_2)| \\
&\leqslant L_3(t)\|\xi_{2,t} - \hat{\xi}_{2,t}\|_1,
\end{aligned} \tag{2.14}$$

where

$$\begin{aligned}
L_3(t) &= \max\{(1-u_1(t))\beta e^{-m\tau_1}|v_1(t-\tau_1)|, (1-u_1(t))\beta e^{-m\tau_1}|v_1(t-\tau_1)|, k|z_1(t-\tau_2)|, k|\hat{y}_1(t-\tau_2)|\} \\
&\quad \times \|\xi_{2,t} - \hat{\xi}_{2,t}\|_1.
\end{aligned}$$

Combining the results in (2.11), (2.13), and (2.14), we obtain

$$\|F(t,\xi_t) - F(t,\hat{\xi}_t)\|_1 \leqslant (L_1(t) + L_2(t))\|\xi_{1,t} - \hat{\xi}_{1,t}\|_1 + L_3(t)\|\xi_{2,t} - \hat{\xi}_{2,t}\|_1.$$

Finally, from Theorems 2.1 and 2.2 all variables are nonegative and bounded, we can replace $L_1(t)$, $L_2(t)$, $L_3(t)$ by upper bounds defined by

$$\begin{aligned}
L_1 &= \max\{\sigma,\ \sigma + 2p + (1-u_{2,\min})a,\ \alpha+\delta,\ \mu,\ h,\ \varepsilon\}, \\
L_2 &= \max\{(1-u_{1,\min})\beta\bar{v},\ q\bar{z},\ ((1-u_{1,\min})\beta\bar{x} + (\gamma+g)\bar{w})\,,\ (\gamma+g)\bar{v},\ q\bar{y}\}, \\
L_3 &= \max\{(1-u_{1,\min})\beta e^{-m\tau_1}\bar{v},\ (1-u_{1,\min})\beta e^{-m\tau_1}\bar{x}\}, k\bar{z}, k\bar{y}\},
\end{aligned} \tag{2.15}$$

where, e.g., $\bar{x}$ means the upper bound on $x(t)$ and $u_{1,\min} \in [0,1]$, and $u_{2,\min} \in [0,1]$ are the minimum values of $u_1(t)$ and $u_2(t)$ for $t \geqslant -\tau$, respectively. Then, using (2.15), we can rewrite (2.10) as the Lipschitz condition

$$\|F(t,\xi_t)) - F(\hat{\xi}_t)\|_1 \leqslant (L_1 + L_2 + L_3)\|\xi_t - \hat{\xi}_t\|_1 = L\|\xi_t - \hat{\xi}_t\|_1.$$

The proof is complete. □

2.4. Equilibrium states

The system (2.1) has three equilibrium states.

1. Infection-free equilibrium point:

$$E_0 = (x_0, y_0, c_0, v_0, w_0, z_0) = \left(\frac{\Lambda}{\sigma}, 0, 0, 0, 0, 0\right).$$

2. Immune-free equilibrium point: $E_1 = (x_1, y_1, c_1, v_1, 0, 0)$, where

$$x_1 = \frac{(\sigma+p)(\alpha+\delta)\mu}{(1-u_1)(1-u_2)\beta e^{-m\tau_1}a\alpha}, \qquad y_1 = \frac{(\alpha+\delta)c_1}{(1-u_2)a},$$
$$c_1 = \frac{\sigma\mu(\sigma+p)(\alpha+\delta)(R_0-1)}{(1-u_1)\beta\alpha\left((\sigma+p)(\alpha+\delta)-p(\alpha+\delta)e^{-m\tau_1}\right)}, \quad v_1 = \frac{\alpha c_1}{\mu},$$

and where

$$R_0 = \frac{(1-u_1)(1-u_2)\beta e^{-m\tau_1}\Lambda a\alpha}{\mu\sigma(\sigma+p)(\alpha+\delta)} \tag{2.16}$$

can be identified as the basic reproduction number (see Subsection 2.5). Note that the infected populations y_1 and c_1 and free virus population v_1 are positive if and only if $R_0 > 1$.

3. Endemic equilibrium point: $(E_2) = (x_2, y_2, c_2, v_2, w_2, z_2)$, where

$$x_2 = \frac{(\Lambda k + p\varepsilon)g}{(\sigma g + (1-u_1)\beta h)k}, \qquad y_2 = \frac{\varepsilon}{k}, \qquad c_2 = \frac{(1-u_2)a\varepsilon}{k(\alpha+\delta)}, \qquad v_2 = \frac{h}{g},$$
$$w_2 = \frac{(1-u_2)a\varepsilon\alpha g}{(\alpha+\delta)\gamma hk} - \frac{\mu}{\gamma}, \qquad z_2 = \frac{(1-u_1)\beta e^{-m\tau_1}khx_2}{qg\varepsilon} - \frac{\sigma+p}{q}.$$

Note that the endemic equilibrium exists if and only if the antibody population w_2 and cytotoxic T-lymphocytes population z_2 are positive.

2.5. The basic reproduction number (R_0)

The basic reproduction number (R_0) is the expected concentration of secondary cases produced when a typical infective hepatocyte (y) enters an infection-free population. To calculate R_0, we use the next-generation method of van den Driessche and Watmough [59]. We obtain

$$\mathcal{F} = \begin{bmatrix} (1-u_1)\beta e^{-m\tau_1}xv \\ 0 \\ 0 \end{bmatrix} \text{ and } \mathcal{V} = \begin{bmatrix} (\sigma+p)y + qzy \\ \alpha c + \delta c - (1-u_2)ay \\ \gamma vw + \mu v - \alpha c \end{bmatrix}.$$

Then we have

$$F = \begin{bmatrix} 0 & 0 & (1-u_1)\beta e^{-m\tau_1}x \\ 0 & 0 & 0 \\ 0 & 0 & 0 \end{bmatrix} \text{ and } V = \begin{bmatrix} (\sigma+p)+qz & 0 & 0 \\ -(1-u_2)a & \alpha+\delta & 0 \\ 0 & -\alpha & \gamma w+\mu \end{bmatrix}.$$

By substituting the infection-free equilibrium point $E_0 = \left(\frac{\Lambda}{\sigma}, 0, 0, 0, 0, 0\right)$ into the Jacobian matrices F and V and computing the inverse V^{-1}, we obtain the next-generation matrix

$$FV^{-1} = \begin{bmatrix} \frac{(1-u_1)(1-u_2)\beta e^{-m\tau_1}\Lambda a\alpha}{\mu\sigma(\sigma+p)(\alpha+\delta)} & \frac{(1-u_1)\beta e^{-m\tau_1}\Lambda\alpha}{\mu\sigma(\sigma+p)(\alpha+\delta)} & \frac{(1-u_1)\beta e^{-m\tau_1}\Lambda}{\sigma\mu} \\ 0 & 0 & 0 \\ 0 & 0 & 0 \end{bmatrix}.$$

The basic reproduction number R_0 is then the maximum eigenvalue $\rho(FV^{-1})$, which is given by equation (2.16). From the next-generation method, $R_0 < 1$ is the condition for local asymptotic stability of the infection-free equilibrium E_0 and, as shown above, $R_0 > 1$ is also the condition for the existence of the immune-free equilibrium E_1.

2.6. Sensitivity analysis

These indices demonstrate the sensitivity of the parameter associated with the basic reproduction number (R_0). It determines whether it increases or decreases the values of the basic reproduction number (R_0) and provides crucial details on the comparative changes in significant parameters. As a result, they support the development of effective strategies for controlling the transmission of HBV.

With sensitivity analysis, we can investigate how each parameter used in the model affects the value of the basic reproduction number. We use the method of normalized forward sensitivity index (see, e.g., Samsuzzoha et al. [56] and Ngoteya et al. [52]), where the normalized forward sensitivity index of the basic reproduction number R_0 with respect to a parameter value h is given by

$$S_h^{R_0} = \frac{h}{R_0}\frac{\partial R_0}{\partial h} = h\frac{\partial \log(R_0)}{\partial h}. \tag{2.17}$$

Note that, the sensitivity index gives an estimate of the relative change in R_0 from a relative change in a parameter h. For example, if h is changed by $\delta h = \nu h$, where $0 < \nu < 1$ is a fraction then, to first-order, the relative change in R_0 is

$$\frac{\delta R_0}{R_0} = \frac{\nu h \frac{\partial R_0}{\partial h}}{R_0} = \nu S_h^{R_0}.$$

Using equations (2.17) and (2.16), we obtain the values of the sensitivity indices shown in Table 2 for the parameters in Table 1.

Table 2: Numerical values of sensitivity indices of R_0.

Parameter	Index at parameter value	Sign
Λ	+1	+ve
β	+1	+ve
m	-0.0220	-ve
τ_1	-0.0220	-ve
a	+1	+ve
u_1	-0.1111	-ve
u_2	-0.1111	-ve
α	0.0574	+ve
σ	-1.0840	-ve
μ	-1	-ve
p	-0.9160	-ve
δ	-0.0574	-ve

From these calculations, we can rank the indices in order of effectiveness in reducing HBV infection. Table 2 shows that increasing the values of parameters $\Lambda, \beta, a, \alpha$ by 10% will increase the values of R_0 by 10%, 10%, 10%, and 0.57%, respectively. On the other hand, Table 2 shows that increasing the values of $m, \tau_1, u_1, u_2, \sigma, \mu, p, \delta$ by 10% will decrease the values of R_0 by 0.22%, 0.22%, 1.11%, 1.11%, 10.84%, 10%, 9.16%, and 0.57%, respectively. Therefore, if we want to reduce R_0, we should focus on increasing the values of σ, μ, and p and reducing the values of Λ, β, and a because these are the factors that are most effective in reducing the infection. It can also be seen that increasing the values of the controls u_1 and u_2 have the same effect as reducing the values of the parameters Λ, β, a, and α, the first three of which are the most effective in reducing the values of R_0.

3. Optimal control

We consider the optimal control of the time delay model for HBV infections defined in Section 2.1. The optimal control problem is as follows:

$$\max_{u_1,u_2} J(u_1,u_2) = \int_0^T f_0(x(t),w(t),z(t),u_1(t),u_2(t))dt, \tag{3.1}$$

where $f_0(x(t),w(t),z(t),u_1(t),u_2(t)) = x(t)+w(t)+z(t)-\frac{1}{2}A_1u_1^2(t)-\frac{1}{2}A_2u_2^2(t)$, $0 \leqslant u_1(t) \leqslant 1$, $0 \leqslant u_2(t) \leqslant 1$, subject to the HBV equations in system (2.1):

$$\begin{aligned}
\frac{dx}{dt} &= f_1(x(t),v(t),y(t),u_1(t)) = \Lambda-\sigma x(t)-(1-u_1(t))\beta x(t)v(t)+py(t),\\
\frac{dy}{dt} &= f_2(y(t),z(t),x(t-\tau_1),v(t-\tau_1),u_1(t))\\
&= (1-u_1(t))\beta e^{-m\tau_1}x(t-\tau_1)v(t-\tau_1)-(\sigma+p)y(t)-qy(t)z(t),\\
\frac{dc}{dt} &= f_3(y(t),c(t),u_2(t)) = (1-u_2(t))ay(t)-(\alpha+\delta)c(t),\\
\frac{dv}{dt} &= f_4(c(t),v(t),w(t)) = \alpha c(t)-\gamma v(t)w(t)-\mu v(t),\\
\frac{dw}{dt} &= f_5(v(t),w(t)) = gv(t)w(t)-hw(t),\\
\frac{dz}{dt} &= f_6(z(t),y(t-\tau_2),z(t-\tau_2)) = ky(t-\tau_2)z(t-\tau_2)-\varepsilon z(t),
\end{aligned} \tag{3.2}$$

with initial conditions

$$\begin{aligned}
&x(t) \geqslant 0, \text{ given } -\tau_1 \leqslant t \leqslant 0, && y(t) \geqslant 0, \text{ given } -\tau_2 \leqslant t \leqslant 0,\\
&c(0) \geqslant 0, && v(t) \geqslant 0, \text{ given } -\tau_1 \leqslant t \leqslant 0,\\
&w(0) \geqslant 0, && z(t) \geqslant 0, \text{ given } -\tau_2 \leqslant t \leqslant 0,
\end{aligned} \tag{3.3}$$

where T is the period of therapy, and A_1 and A_2 are measures of the relative costs of the interventions associated with the controls u_1 and u_2, respectively. The expression $\frac{A_1u_1^2}{2}$ represents cost associated with $u_1(t)$ and $\frac{A_2u_2^2}{2}$ represents cost associated with $u_2(t)$. The two control functions, $u_1(t)$ and $u_2(t)$ are assumed to be bounded and Lebesgue integrable. We have assumed a quadratic cost for administering the controls u_1 and u_2 for two reasons. Firstly, there are typically increasing costs with reaching higher fractions of a population. The quadratic is the simplest nonlinear function and therefore we have used it in our model. Secondly, assuming a linear cost for the control leads to a "bang-bang" solution, where the solution is always to maximize or minimize the drug cost at each point in time. Our target is to maximize the objective functional defined in equation (3.1) by increasing the number of the uninfected hepatocytes $x(t)$, the antibodies $w(t)$ and the CTLs immune responses $z(t)$ and decreasing the viral load for minimum therapy cost, i.e., we are finding the optimal control pair (u_1^*,u_2^*) such that

$$J(u_1^*,u_2^*) = \max_{(u_1,u_2)\in U} J(u_1,u_2),$$

where the control set U is defined by

$$U = \{(u_1(t),u_2(t)) : u_i(t) \text{ measurable } 0 \leqslant u_i(t) \leqslant 1, t \in [0,T], i = 1,2\}. \tag{3.4}$$

3.1. Existence of an optimal control pair

The following theorem proves the existence of an optimal control pair. The proof is based on a result of Fleming and Rishel [21] which is based on a theorem of Cesari [12].

Theorem 3.1. *There exists an optimal control pair* $(u_1^*, u_2^*) \in U$ *such that*

$$J(u_1^*, u_2^*) = \max_{(u_1,u_2)\in U} J(u_1, u_2).$$

Proof. To use the result of Fleming and Rishel [21], we need to check the following properties.

- (P_1) The set of state variables and controls is nonempty.
- (P_2) The set of controls (U) is closed and convex.
- (P_3) The right hand side of the state system is bounded by a linear function in the state and control variables.
- (P_4) The integrand of the objective functional is concave on U.
- (P_5) There exists a constant $\zeta > 1$ and positive numbers η_1, $\eta_2 > 0$, such that the integrand $I(x, w, z, u_1, u_2)$ of the objective functional satisfies

$$I(x, w, z, u_1, u_2) \leqslant \eta_1 - \eta_2(|u_1|^2 + |u_2|^2)^{\frac{\zeta}{2}},$$

where $I(x, w, z, u_1, u_2) = x(t) + w(t) + z(t) - \left(\frac{A_1}{2}u_1^2(t) + \frac{A_2}{2}u_2^2(t)\right)$.

The proofs that our model satisfies the conditions are as follows.

- (P_1) From Theorem 2.3, the solution of the system (2.1) exists and is unique for given initial conditions and given controls in the set U. Therefore, the set of state variables and controls is nonempty and condition P_1 is satisfied.
- (P_2) The control set U defined in (3.4) is clearly convex and closed.
- (P_3) From Theorem 2.3, the right-hand-side of (2.1) is bounded by a linear function in the state and control variables.
- (P_4) The integrand of the objective functional in (3.1) is clearly concave on U.
- (P_5) Since, from Theorem 2.2, $x(t) \leqslant \bar{x}$, $w(t) \leqslant \bar{w}$, $z(t) \leqslant \bar{z}$ are bounded above, and A_1, $A_2 > 0$, we have

$$\begin{aligned} I(x, w, z, u_1, u_2) &= x(t) + w(t) + z(t) - \left(\frac{A_1}{2}u_1^2(t) + \frac{A_2}{2}u_2^2(t)\right) \\ &\leqslant \bar{x} + \bar{w} + \bar{z} - \frac{1}{2}\min\{A_1, A_2\}(u_1^2(t) + u_2^2(t)) = \eta_1 - \eta_2(|u_1|^2 + |u_2|^2)^{\frac{\zeta}{2}}, \end{aligned}$$

where $\eta_1 = \bar{x} + \bar{w} + \bar{z}$, $\eta_2 = \frac{1}{2}\min\{A_1, A_2\}$, and $\zeta = 2$.

This completes the proof. □

3.2. Pontryagin maximum principle

Derivations of the Pontryagin maximum principle can be found in many books and papers for both no-delay problems (see, e.g., [42, 44, 55]) and for time delay problems (see, e.g., [22, 24, 34, 37]). In this section, we will summarize the necessary conditions that the Pontryagin maximum principle gives for the solution of the time delay optimal control problem of equations (3.1), (3.2), and (3.3).

The Hamiltonian for the system (3.1) and (3.2) is given by

$$\begin{aligned} &H(\mathbf{x}(t), x(t-\tau_1), y(t-\tau_2), v(t-\tau_1), z(t-\tau_2), u_1(t), u_2(t), \lambda(t)) \\ &\quad = f_0(x(t), w(t), z(t), u_1(t), u_2(t)) + \lambda_1(t)f_1(x(t), v(t), y(t), u_1(t)) \\ &\qquad + \lambda_2(t)f_2(y(t), z(t), x(t-\tau_1), v(t-\tau_1), u_1(t)) \\ &\qquad + \lambda_3(t)f_3(y(t), c(t), u_2(t)) + \lambda_4(t)f_4(c(t), v(t), w(t)) \\ &\qquad + \lambda_5(t)f_5(v(t), w(t)) + \lambda_6(t)f_6(z(t), y(t-\tau_2), z(t-\tau_2)), \end{aligned}$$

where, for ease of writing, we define

$$\mathbf{x}(t) = (x_1(t), x_2(t), x_3(t), x_4(t), x_5(t), x_6(t))^T \tag{3.5}$$

with $x_1(t) = x(t)$, $x_2(t) = y(t)$, $x_3(t) = c(t)$, $x_4(t) = v(t)$, $x_5(t) = w(t)$, $x_6(t) = z(t)$, and $\lambda(t)$

$= (\lambda_1(t), \lambda_2(t), \lambda_3(t), \lambda_4(t), \lambda_5(t), \lambda_6(t))^T$.

Following the definitions of the costate equations in Forde et al. [22], we separate the costate equations into 3 types: 1) no time delay; 2) time delay τ_1; and 3) time delay τ_2.

1. No time delay: Since the state variables $x_3(t) = c(t)$ and $x_5(t) = w(t)$ have no time delay, the costate equations for $\lambda_3(t)$ and $\lambda_5(t)$ are as follows:

$$\begin{aligned}
\dot{\lambda}_3(t) &= -\frac{\partial H(\mathbf{x}(t), x(t-\tau_1), y(t-\tau_2), v(t-\tau_1), z(t-\tau_2), u_1(t), u_2(t), \lambda(t))}{\partial c(t)} \\
&= -\lambda_3(t)\frac{\partial f_3(y(t), c(t), u_2(t))}{\partial c(t)} - \lambda_4(t)\frac{\partial f_4(c(t), v(t), w(t))}{\partial c(t)} = (\alpha+\delta)\lambda_3(t) - \alpha\lambda_4(t).
\end{aligned} \tag{3.6}$$

$$\begin{aligned}
\dot{\lambda}_5(t) &= -\frac{\partial H(\mathbf{x}(t), x(t-\tau_1), y(t-\tau_2), v(t-\tau_1), z(t-\tau_2), u_1(t), u_2(t), \lambda(t))(t))}{\partial w(t)} \\
&= -\frac{\partial f_0(x(t), w(t), z(t), u_1(t), u_2(t))}{\partial w(t)} - \lambda_4(t)\frac{\partial f_4(c(t), v(t), w(t))}{\partial w(t)} - \lambda_5(t)\frac{\partial f_5(v(t), w(t))}{\partial w(t)} \\
&= -1 + \lambda_4(t)\gamma v(t) - \lambda_5(t)(gv(t) - h).
\end{aligned} \tag{3.7}$$

The time interval for the two costate equations is $0 \leqslant t \leqslant T$ with the boundary conditions $\lambda_3(T) = \lambda_5(T) = 0$.

2. Time delay τ_1: The state variable $x_1(t) = x(t)$ also has a time delay term $x(t-\tau_1)$ and the variable $x_4(t) = v(t)$ also has a time delay term $v(t-\tau_1)$. Therefore, the costate equations for $\lambda_1(t)$ and $\lambda_4(t)$ are defined separately for the time intervals $0 \leqslant t \leqslant T-\tau_1$ and $T-\tau_1 \leqslant t \leqslant T$. The time delay equations for $\lambda_1(t)$ are given by

$$\begin{aligned}
\dot{\lambda}_1(t) &= -\frac{\partial H(\mathbf{x}(t), x(t-\tau_1), y(t-\tau_2), v(t-\tau_1), z(t-\tau_2), u_1(t), u_2(t), \lambda(t))}{\partial x(t)} \\
&\quad - \frac{\partial H(\mathbf{x}(t+\tau_1), x(t), y(t+\tau_1-\tau_2), v(t), z(t+\tau_1-\tau_2), u_1(t+\tau_1), u_2(t+\tau_1), \lambda(t+\tau_1))}{\partial x(t)} \\
&= -\frac{\partial f_0(x(t), w(t), z(t), u_1(t), u_2(t))}{\partial x(t)} - \lambda_1(t)\frac{\partial f_1(x(t), v(t), y(t), u_1(t))}{\partial x(t)} \\
&\quad - \lambda_2(t+\tau_1)\frac{\partial f_2(y(t+\tau_1), z(t+\tau_1), x(t), v(t), u_1(t+\tau_1))}{\partial x(t)} \\
&= -1 + \lambda_1(t)(\sigma + (1-u_1(t))\beta v(t)) - \lambda_2(t+\tau_1)(1-u_1(t+\tau_1))\beta e^{-m\tau_1} v(t),
\end{aligned} \tag{3.8}$$

for $0 \leqslant t \leqslant T-\tau_1$ and

$$\begin{aligned}
\dot{\lambda}_1(t) &= -\frac{\partial H(\mathbf{x}(t), x(t-\tau_1), y(t-\tau_2), v(t-\tau_1), z(t-\tau_2), u_1(t), u_2(t), \lambda(t))}{\partial x(t)} \\
&= -1 + \lambda_1(t)(\sigma + (1-u_1(t))\beta v(t)),
\end{aligned}$$

for $T-\tau_1 \leqslant t \leqslant T$.The time delay equations for $\lambda_4(t)$ are given by

$$\begin{aligned}
\dot{\lambda}_4(t) &= -\frac{\partial H(\mathbf{x}(t), x(t-\tau_1), y(t-\tau_2), v(t-\tau_1), z(t-\tau_2), u_1(t), u_2(t), \lambda(t))}{\partial v(t)} \\
&\quad - \frac{\partial H(\mathbf{x}(t+\tau_1), x(t), y(t+\tau_1-\tau_2), v(t), z(t+\tau_1-\tau_2), u_1(t+\tau_1), u_2(t+\tau_1), \lambda(t+\tau_1))}{\partial v(t)} \\
&= -\lambda_1(t)\frac{\partial f_1(x(t), v(t), y(t), u_1(t))}{\partial v(t)} - \lambda_4(t)\frac{\partial f_4(c(t), v(t), w(t))}{\partial v(t)} - \lambda_5(t)\frac{\partial f_5(v(t), w(t))}{\partial v(t)} \\
&\quad - \lambda_2(t+\tau_1)\frac{\partial f_2(y(t+\tau_1), z(t+\tau_1), x(t), v(t), u_1(t+\tau_1))}{\partial v(t)} \\
&= \lambda_1(t)(1-u_1(t))\beta x(t) + \lambda_4(t)(\gamma w(t) + \mu) - \lambda_5(t) g w(t) \\
&\quad - \lambda_2(t+\tau_1)(1-u_1(t+\tau_1))\beta e^{-m\tau_1} x(t),
\end{aligned} \tag{3.9}$$

for $0 \leqslant t \leqslant T - \tau_1$, and

$$\begin{aligned}\dot{\lambda}_4(t) &= -\frac{\partial H(\mathbf{x}(t), x(t-\tau_1), y(t-\tau_2), v(t-\tau_1), z(t-\tau_2), u_1(t), u_2(t), \lambda(t))}{\partial v(t)} \\ &= \lambda_1(t)(1-u_1(t))\beta x(t) + \lambda_4(t)(\gamma w(t) + \mu) - \lambda_5(t) g w(t)\end{aligned}$$

for $T - \tau_1 \leqslant t \leqslant T$. The conditions on the costate equations are continuity of $x(t)$ and $v(t)$ at $t = T - \tau_1$ and $\lambda_1(T) = \lambda_4(T) = 0$.

3. Time delay τ_2: The state variable $x_2(t) = y(t)$ also has a time delay term $y(t-\tau_2)$ and the variable $x_6(t) = z(t)$ also has a time delay term $z(t-\tau_2)$. Therefore, the costate equations for $\lambda_2(t)$ and $\lambda_6(t)$ are defined separately for the time intervals $0 \leqslant t \leqslant T - \tau_2$ and $T - \tau_2 \leqslant t \leqslant T$.

The time delay equations for $\lambda_2(t)$ are given by

$$\begin{aligned}\dot{\lambda}_2(t) = &-\frac{\partial H(\mathbf{x}(t), x(t-\tau_1), y(t-\tau_2), v(t-\tau_1), z(t-\tau_2), u_1(t), u_2(t), \lambda(t))}{\partial y(t)} \\ &- \frac{\partial H(\mathbf{x}(t+\tau_2), x(t-\tau_1+\tau_2), y(t), v(t-\tau_1+\tau_2), z(t), u_1(t+\tau_2), u_2(t+\tau_2), \lambda(t+\tau_2))}{\partial y(t)} \\ &- \lambda_1(t)\frac{\partial f_1(x(t), v(t), y(t), u_1(t))}{\partial y(t)} - \lambda_2(t)\frac{\partial f_2(y(t), z(t), x(t-\tau_1), v(t-\tau_1), u_1(t))}{\partial y(t)} \\ &- \lambda_3(t)\frac{\partial f_3(y(t), c(t), u_2(t))}{\partial y(t)} - \lambda_6(t+\tau_2)\frac{\partial f_6(z(t+\tau_2), y(t), z(t))}{\partial y(t)} \\ = &-\lambda_1(t)p + \lambda_2(t)(\sigma + p + qz(t)) - \lambda_3(t)a(1-u_2(t)) - \lambda_6(t+\tau_2)kz(t),\end{aligned} \tag{3.10}$$

for $0 \leqslant t \leqslant T - \tau_2$ and

$$\begin{aligned}\dot{\lambda}_2(t) = &-\frac{\partial H(\mathbf{x}(t), x(t-\tau_1), y(t-\tau_2), v(t-\tau_1), z(t-\tau_2), u_1(t), u_2(t), \lambda(t))}{\partial y(t)} \\ &- \lambda_1(t)p + \lambda_2(t)(\sigma + p + qz(t)) - \lambda_3(t)a(1-u_2(t)),\end{aligned}$$

for $T - \tau_2 \leqslant t \leqslant T$. The time delay equations for $\lambda_6(t)$ are given by

$$\begin{aligned}\dot{\lambda}_6(t) = &-\frac{\partial H(\mathbf{x}(t), x(t-\tau_1), y(t-\tau_2), v(t-\tau_1), z(t-\tau_2), u_1(t), u_2(t), \lambda(t))}{\partial z(t)} \\ &- \frac{\partial H(\mathbf{x}(t+\tau_2), x(t-\tau_1+\tau_2), y(t), v(t-\tau_1+\tau_2), z(t), u_1(t+\tau_2), u_2(t+\tau_2), \lambda(t+\tau_2))}{\partial z(t)} \\ = &-\frac{\partial f_0(x(t), w(t), z(t), u_1(t), u_2(t))}{\partial z(t)} - \lambda_2(t)\frac{\partial f_2(y(t), z(t), x(t-\tau_1), v(t-\tau_1), u_1(t))}{\partial z(t)} \\ &- \lambda_6(t)\frac{\partial f_6(z(t), y(t-\tau_2), z(t-\tau_2))}{\partial z(t)} - \lambda_6(t+\tau_2)\frac{\partial f_6(z(t+\tau_2), y(t), z(t))}{\partial z(t)} \\ = &-1 + \lambda_2(t)qy(t) + \varepsilon\lambda_6(t) - \lambda_6(t+\tau_2)ky(t)\end{aligned} \tag{3.11}$$

for $0 \leqslant t \leqslant T - \tau_2$, and

$$\begin{aligned}\dot{\lambda}_6(t) &= -\frac{\partial H(\mathbf{x}(t), x(t-\tau_1), y(t-\tau_2), v(t-\tau_1), z(t-\tau_2), u_1(t), u_2(t), \lambda(t))}{\partial z(t)} \\ &= -1 + \lambda_2(t)qy(t) + \varepsilon\lambda_6(t), \quad \text{for } T - \tau_2 \leqslant t \leqslant T.\end{aligned}$$

The conditions on the costate equations are continuity of $y(t)$ and $z(t)$ at $t = T - \tau_2$ and $\lambda_2(T) = \lambda_6(T) = 0$.

3.3. Maximum control values

In the Pontryagin maximum principle, the optimal values of the state and costate variables $\mathbf{x}^*(t)$ and $\lambda^*(t)$ values occur for values of $u_1^*(t)$ and $u_2^*(t)$ which give local maximum values of the Hamiltonian. For the case of bounded controls with a concave Hamiltonian, there are 3 differerent possibilities.

1. An internal point of $0 \leqslant u_1(t) \leqslant 1$ or $0 \leqslant u_2(t) \leqslant 1$. For $u_1(t)$, the condition is:

$$\begin{aligned} 0 &= \frac{\partial H(\mathbf{x}^*(t), x^*(t-\tau_1), y^*(t-\tau_2), v^*(t-\tau_1), z^*(t-\tau_2), u_1(t), u_2(t), \lambda^*(t))}{\partial u_1(t)} \\ &= \frac{\partial f_0(x^*(t), w^*(t), z^*(t), u_1(t), u_2(t))}{\partial u_1(t)} + \lambda_1(t)\frac{\partial f_1(x^*(t), v^*(t), y^*(t), u_1(t))}{\partial u_1(t)} \\ &\quad + \lambda_2^*(t)\frac{\partial f_2(y^*(t), z^*(t), x^*(t-\tau_1), v^*(t-\tau_1), u_1(t))}{\partial u_1(t)} \\ &= -A_1 u_1(t) + \lambda_1^*(t)\beta x^*(t)v^*(t) - \lambda_2^*(t)\beta e^{-m\tau_1}x^*(t-\tau_1)v^*(t-\tau_1). \end{aligned}$$

Therefore, a possible internal point for the first control is:

$$\bar{u}_1(t) = \frac{\beta}{A_1}\big(\lambda_1^*(t)x^*(t)v^*(t) - \lambda_2^*(t)e^{-m\tau_1}x^*(t-\tau_1)v^*(t-\tau_1)\big).$$

This is a maximum point of H since $\frac{\partial^2 H}{\partial u_1^2} = -A_1 < 0$ and H is a concave function of u_1. For $u_2(t)$, the condition is:

$$\begin{aligned} 0 &= \frac{\partial H(\mathbf{x}(t), x(t-\tau_1), y(t-\tau_2), v(t-\tau_1), z(t-\tau_2), u_1(t), u_2(t), \lambda(t))}{\partial u_2(t)} \\ &= \frac{\partial f_0(x(t), w(t), z(t), u_1(t), u_2(t))}{\partial u_2(t)} + \lambda_3(t)\frac{\partial f_3(y(t), c(t), u_2(t))}{\partial u_2(t)} \\ &= -A_2 u_2(t) - \lambda_3(t)\alpha y(t). \end{aligned}$$

Therefore, a possible internal point for the second control is:

$$\bar{u}_2(t) = -\frac{1}{A_2}\lambda_3^*(t)\alpha y^*(t).$$

This is a maximum point of H since $\frac{\partial^2 H}{\partial u_2^2} = -A_2 < 0$ and H is a concave function of u_2.

2. At lower bounds $u_1(t) = 0$ or $u_2(t) = 0$.

3. At upper bounds $u_1(t) = 1$ or $u_2(t) = 1$.

There are therefore 9 possible choices for the optimal control pair $(u_1^*(t), u_2^*(t))$. In summary.

1. If the internal point $\bar{u}_1(t) \in [0,1]$, then $u_1^*(t) = \bar{u}_1(t)$ is the maximum point. If $\bar{u}_1(t) < 0$, then $u_1^*(t) = 0$ is the maximum point. If $\bar{u}_1(t) > 1$, then $u_1^*(t) = 1$ is the maximum point. This is written in the literature as $u_1^*(t) = \max(0, \min(1, \bar{u}_1(t))$.
2. If the internal point $\bar{u}_2(t) \in [0,1]$, then $u_2^*(t) = \bar{u}_2(t)$ is the maximum point. If $\bar{u}_2(t) < 0$, then $u_2^*(t) = 0$ is the maximum point. If $\bar{u}_2(t) > 1$, then $u_2^*(t) = 1$ is the maximum point. This is written in the literature as $u_2^*(t) = \max(0, \min(1, \bar{u}_2(t))$.

3.4. Algorithm for solution of the optimal control problem

The algorithm that we use to compute the optimal controls with Matlab is as follows.

1. Select an initial feasible control pair $(u_1^{(0)}(t), u_2^{(0)}(t))$.
   For $k = 0, 1, \ldots, k_{max}$:

(a) for the given initial conditions and the given control pair, integrate the system of state equations (2.1) using an ODE delay solver such as *dde23* in Matlab;
(b) since the costate equations (3.6)-(3.11) defined in the Pontryagin maximum principle section 3.2 must be integrated in the backwards direction in time for numerical stability, time-reverse the system of costate equations, and then integrate the time-reversed system of costate equations in the forward direction using the same ODE solver *dde23* as for the state equations;
(c) use the methods described in section 3.3 to find the values of the new control pair $(u_1^{(k+1)}(t), u_2^{(k+1)}(t))$ that maximize the Hamiltonian for the given values of $\mathbf{x}(t)$ and $\lambda(t)$ obtained from the state and costate integrations in (a) and (b);
(d) compare the new control pair $(u_1^{(k+1)}(t), u_2^{(k+1)}(t))$ with the previous control pair $(u_1^{(k)}(t), u_2^{(k)}(t))$.

2. If the two control pairs are the same to a specified tolerance stop. Otherwise replace $(u_1^{(k)}(t), u_2^{(k)}(t))$ by $(u_1^{(k+1)}(t), u_2^{(k+1)}(t))$ and repeat steps (a), (b), (c), and (d) for the new control pair.

Note: A much simpler delayed optimal control problem has been considered by Ibrahim et al. [34]. In their paper, the model involved only one state equation and one time-delayed optimal control. The algorithm used in their paper is similar to the algorithm above, with the exception that an EOSM step method is used to solve the state equations forward in time and the costate equations backward in time. The EOSM step method used in the integrations in the Ibrahim et al. paper appear to be based on an implicit Taylor series method of specified order. In our algorithm, we have used the Matlab *dde23* function which is based on a second-order Runge-Kutta method with a 3rd-order corrector term and which automatically adjusts the step size to attain a desired accuracy.

4. Numerical results

We begin by looking at the solutions of system (2.1) for zero controls $u_1 = u_2 = 0$ for the zero delay case and for the nonzero delay cases : $\tau_1 = 2$ days for the delay in the production of infected hepatocytes by free virus and $\tau_2 = 4$ days for the delay in the antigenic stimulation generating CTLs. We then look at the optimal control problem (3.1) for system (2.1) for the nonzero delay cases.

In the numerical simulations, we have used the values of the parameters given in Table 1, i.e., $\Lambda = 1$, $\sigma = 0.011$, $\beta = 0.0014$, $p = 0.012$, $m = 0.011$, $q = 0.001$, $a = 0.15$, $\alpha = 0.87$, $\mu = 0.693$, $g = 0.008$, $h = 0.15$, $k = 0.001$,$\varepsilon = 0.5$. As noted in Table 1, the values have been selected from published sources, if available, or reasonable values have been assumed for parameters if no published values could be found.

4.1. Numerical simulations for zero control

The numerical results for the zero delay and nonzero delay cases for zero control are shown in Figures 2 (a)-(f). In all figures, the zero delay results are plotted as blue dashed lines and the nonzero delay results as red solid lines.

Figure 2 (a) shows that the concentration of uninfected hepatocytes (x) with nonzero delay declines faster than the concentration with zero delay during the first 30 days, whereas the concentration with zero delay decreases faster than the nonzero delay from the 30th to the 80th day when both cases reach the same value. The reason for this behavior can be seen in the different infection rates of hepatocytes shown in Figure 2 (b) for the zero and nonzero delay cases. Figure 2 (b) shows that for zero delay the concentration of infected hepatocytes (y) has an initial peak of 1950 cells/ml at 3 days, a second peak of 900 cells/ml at 40 days, a third peak of 330 cells/ml at 100 days and then decreases to a small equilibrium value. For the nonzero delay case, the concentration has a higher initial peak of approximately 3100 cells/ml at 13 days and then a much smaller second peak of 520 cells/ml at 88 days before decreasing to an equilibrium level similar to that of the zero delay case. A possible reason for the much slower initial infection rate in the nonzero delay case is that the delay $\tau_1 = 2$ days slows down the initial growth rate

of the infection. In both cases, the second peak is lower than the first peak. A possible explanation is that the high number of infections in the first peak causes rapid increases in the concentrations of antibodies and CTLs (see Figures 2 (e) and (f)) which then help to reduce the concentrations of infected hepatocytes in the later peaks.

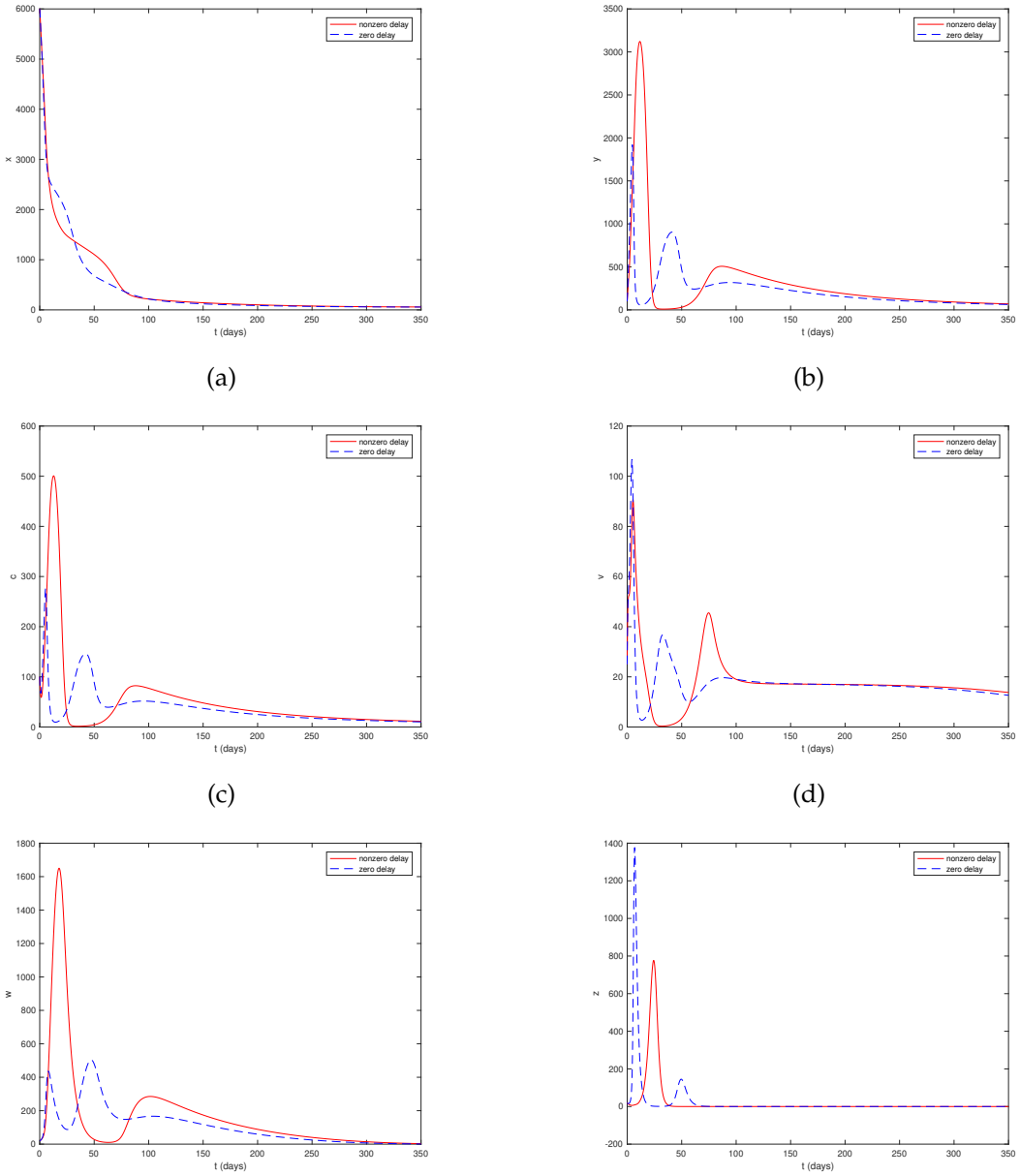

Figure 2: Dynamics of the HBV model (2.1) with zero delay (dashed curves) and with nonzero delay (solid curves) for $\tau_1 = 2$ and $\tau_2 = 4$. (a) Concentration of uninfected hepatocytes (x). (b) Concentration of infected hepatocytes (y). (c) Concentration of intracellular HBV DNA-containing capsids (c). (d) Concentration of free viruses (v). (e) Concentration of antibodies (w) and (f) Concentration of CTLs (z).

Figure 2 (c) for the intracellular HBV DNA-containing capsids (c) shows a similar dynamical pattern to the pattern of the infected hepatocytes for both zero and nonzero delay cases. For zero delay, the concentration of capsids rises to an intial peak of 280 cells/ml at 10 days, a second peak of 150 cells/ml at

45 days and a third peak of 50 cells/ml at 100 days. For nonzero delay, the concentration rises to a high initial peak of 500 cells/ml at 13 days and a second peak of 85 cells/ml at 88 days. Finally, in both cases the concentrations decay at similar rates to equilibrium values. Figure 2 (d) for the free viruses (v) again shows a similar dynamical pattern to the patterns for the infected hepatocytes and the capsids for both zero and nonzero delay cases. For zero delay the concentration of free viruses rises to an intial peak of 105 cells/ml at 5 days and a second peak of 37 cells/ml at 35 days. For nonzero delay, the concentration initially rises to an initial peak of 90 cells/ml at 7 day and a second peak of 47 cells/ml at 78 days. Finally, in both cases the concentrations decay at similar rates to equilibrium values. Figure 2 (e) for the antibodies (w) again shows a similar dynamical pattern to the patterns for the infected hepatocytes, capsids and free viruses for both zero and nonzero delay cases. For zero delay, the concentration rises to an intial peak of 422 cells/ml at 8 days, a second peak of 500 cells/ml at 50 days and a third peak of 190 cells/ml at 100 days. For nonzero delay, the concentration rises to an initial peak of 1650 cells/ml at 18 days and a second peak of 300 cells/ml at 100 days. Finally, in both cases the concentrations decay at similar rates to equilibrium values. As noted above, it can be seen that the pattern of the concentration of antibodies are in the same pattern as the concentration of the infected hepatocytes, capsids and free viruses. However, the peaks in the antibodies occur after the peaks in the infections as the antibodies occur as a response to the infections.

Finally, Figure 2 (f) for the CTLs (z) again shows a similar dynamical pattern to the patterns for the infected hepatocytes, capsids, free viruses and antibodies for both zero and nonzero delay cases. For zero delay, the concentration of CTLs has an initial peak of 1390 cells/ml at 8 days and a second peak of 135 cells/ml at 50 days. For nonzero delay, the concentration of CTLs has only one peak of 790 cells at 25 days. In both cases the concentrations reduce to zero equilibrium value. As for the antibodies, the peaks in the CTLs occur after the peaks in the infections.

In summary, it can be seen that the presence of the delay causes the initial peaks to occur later than in the zero delay case and that the initial peaks of the concentrations are much higher than the later peaks in both cases. The reduction in peak size of the concentrations of infected hepatocytes, capsids and free viruses is almost certainly due to the increased concentrations of antibodies and CTLs resulting from the initial infections.

4.2. Numerical simulations for optimal control

In the simulations, we computed numerical results for nonzero time delays for the two cases of zero control and optimal nonzero control.

The numerical results for the zero control and optimal control cases are shown in Figures 3 (a)-(h) for the time delays $\tau_1 = 2$ days and $\tau_2 = 4$ days. We assumed that control u_1, the efficiency of drug therapy in blocking new infection, and the control u_2, the efficiency of drug therapy in inhibiting viral production, were both in the range $[0, 0.7]$. In all figures, the zero control results are plotted as a blue dashed line and the optimal control results are plotted as a red solid line.

Figures 3 (a) and (b) show the optimal control treatment strategies for u_1 and u_2, respectively. For u_1, the optimal strategy is to initially administer the drug at the maximum allowed efficiency level of 70% until day 149 and then gradually reduce the level towards zero by the final day 350. For u_2, the optimal strategy is to initially administer the drug at the maximum allowed efficiency level of 70% until day 107 and then rapidly reduce the level to zero by day 135. Figures 3 (c)-(h) compare the concentrations of the populations for a period of 350 days for zero control and for the optimal controls shown in Figures 3 (a) and (b). Figure 3 (c) shows that for the parameter values considered in this simulation, the effect of applying the two control variables at the optimal efficiency levels shown in Figues 3 (a) and (b) is to reduce the rate of infection of the uninfected hepatocytes (x) at a much slower rate than for the zero control case until the rates become approximately equal after 250 days. However, as shown in Figures 3 (a) and (b), at 250 days the optimal levels of u_1 and u_2 are both zero.

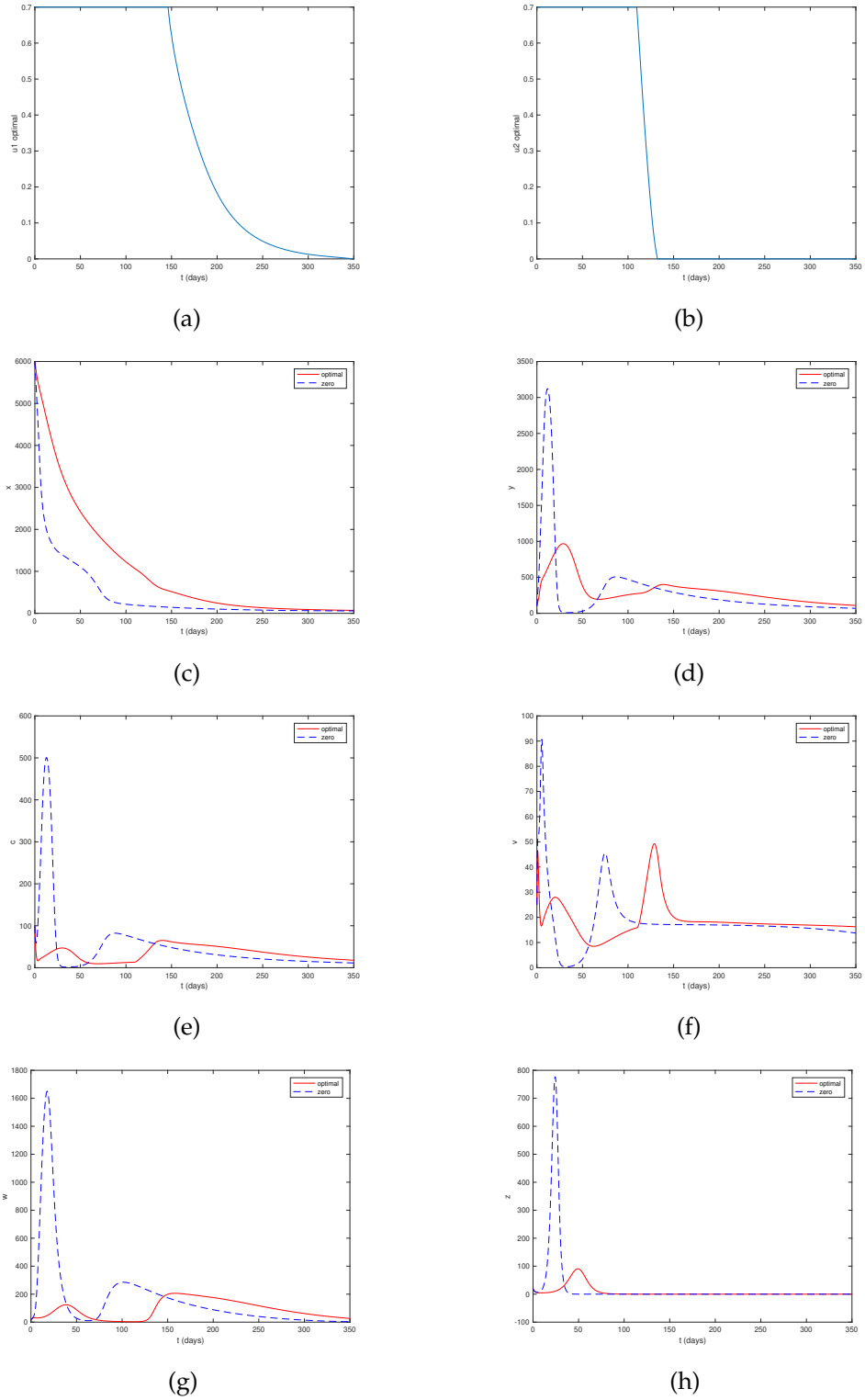

Figure 3: Dynamics of the HBV model (2.1) with both controls (solid curves) and without controls (dashed curves) for time delays $\tau_1 = 2$ and $\tau_2 = 4$. (a) Optimal value of u_1, efficiency of drug therapy in blocking new infection. (b) Optimal value of u_2, efficiency of drug therapy in inhibiting viral production. (c) Concentration of uninfected hepatocytes (c). (d) Concentration of infected hepatocytes (y). (e) Concentration of intracellular HBV DNA-containing capsids (c). (f) Concentration of free viruses (v). (g) Concentration of antibodies (w) and (h) Concentration of CTLs (z).

Figure 3 (d) shows that the concentration of infected hepatocytes (y) increases rapidly in the absence of controls u_1 and u_2 to 3100 cells/ml at 11 days and then declines sharply before rising to a small peak of approximately 500 cells/ml at 86 day. A possible explanation for the second peak being smaller is

that the high levels of y in the first peak lead to a high concentration of CTLs which can help reduce the concentration of infected hepatocytes in the second peak. For the optimal controls, the concentration reaches a peak at approximately 970 cells/ml at 29 days showing the effectiveness of the therapy. As for the uninfected hepatocytes, the peak in the infected hepatocytes at approximately 200 days shows the increase in infection when the rate at which the drugs are administered is reduced.

Figure 3 (e) shows the same dynamical patterns for the concentration of intracellular HBV DNA-containing capsids (c) as the patterns for the infected hepatocytes. That is, for zero controls the concentration increases rapidly to a peak of 500 cells/ml at 12 days, then decreases rapidly to near zero and then rises to a second peak of 80 cells/ml at 86 days. With the optimal controls, the concentration increases more slowly to an initial peak of 44 cells/ml at 30 days and then to a second peak of 60 cells/ml at approximately 140 days. The increase in the second peak for the optimal control can be associated with the reproduction in the drug therapies at 140 days. These results indicate that the control drugs significantly reduce the concentration of intracellular HBV DNA-containing capsids. Since intracellular HBV DNA-containing capsids play a role in the virus life cycle, as they assemble around viral reverse transcriptase, this reduction in them leads to a reduction in the concentration of free viruses as shown in Figure 3 (f).

Figure 3 (f) shows similar dynamical patterns for the concentrations of free viruses (v) as for the capsids (c) in Figure 3 (e). For zero controls, the concentration increases rapidly to a peak of 90 cells/ml at 6 days, then decreases rapidly to near zero and then rises again to a second peak of 45 cells/ml at 74 days. With the optimal controls, the concentration increases more slowly to an initial peak of 28 cells/ml at 20 days and then to a second peak of 49 cells/ml at 126 days. The increase in the second peak for the optimal control can be associated with the reduction in the drug therapies at 126 days.

Figure 3 (g) again shows similar dynamical patterns for the concentrations of antibodies (w). For zero controls, the concentration increases rapidly to a peak of 1640 cells/ml at 16 days, then decreases rapidly to near zero and then rises again to a second peak of 290 cells/ml at 101 days. With the optimal controls, the concentration increases more slowly to an initial peak of 130 cells/ml at 39 days and then to a second peak of 222 cells/ml at 150 days. The increase in the second peak for the optimal control can again be associated with the reduction in the drug therapies at 150 days.

Figure 3 (h) again shows similar dynamical patterns for the concentrations of CTLS (z). For zero control, the concentration of CTLs (z) increases rapidly to a peak of 790 cells/ml at 24 days and then decreases rapidly to zero. For the optimal controls, the concentration rises to a small peak of 89 cells/ml at 49 days and then also decreases to zero.

In general, the results show that the therapy greatly reduces the level of infection. This effect can also be seen from the value of the integral for the state variables $\int_0^{350}(x(t)+w(t)+z(t))dt$, which has a value of 393190 cells/ml for the optimal control case and a value of 220630 cells/ml for the zero control case. The results in Figures 3 (d)-(h) clearly show the effectiveness of the controls in producing a large reduction in the concentration of infected hepatocytes, intracellular HBV DNA-containing capsids, free viruses, and antibodies and therefore to a reduction in the concentration of antibodies and CTLs.

4.3. Numerical simulation of basic reproduction number against controls

In this section, we show the relationship between the values of the optimal controls and the basic reproduction number for the cases of zero delays and nonzero delays.

Figures 4 (a) and (b) show, respectively, the dynamical behavior of R_0 vs time when both controls are in the optimal states shown in Figures 3 (a) and (b) for the zero delay case and nonzero delay case. In both cases, it can be seen that when the controls are set at their maximum allowed level of effectiveness ($u_1 = u_2 = 0.7$), the values of R_0 are a minimum and therefore the rate of reduction in the infected populations will be a maximum. However, as the level of the controls is reduced, the value of R_0 increases and the rate of reduction of the infected populations becomes slower. Near the end of the period of 350 days, the control levels are reduced to zero and R_0 becomes greater than 1 showing that the infection will begin to increase. The results show that the control levels should be maintained at a nonzero minimum level to keep $R_0 < 1$.

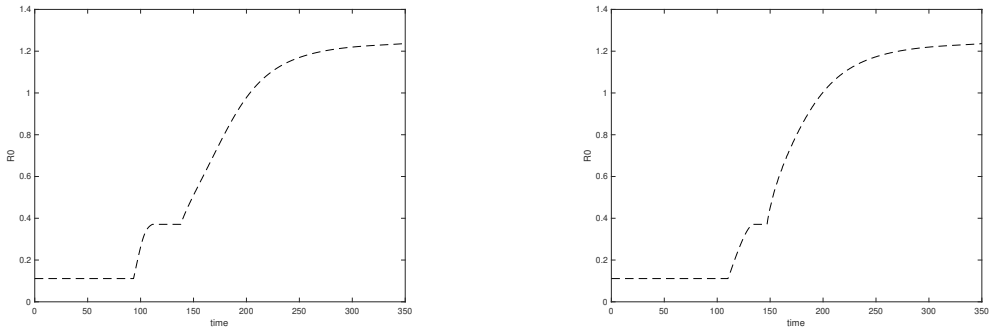

(a) (b)

Figure 4: Plots of basic reproductive number vs time for optimal levels of effectiveness of u_1 and u_2 (see Figures 3 (a) and (b)). (a) Zero time delays. (b) Nonzero time delays: $\tau_1 = 2$ days, $\tau_2 = 4$ days.

Figures 5 and 6 show a comparison between the values of the basic reproductive number for zero delay and nonzero delay cases $\tau_1 = 2$ days and $\tau_2 = 4$ days for a range of values of the controls u_1 and u_2. It can be seen that R_0 increases with time slower in the delay case than in the nondelay case. A comparison of Figure 5 (a) for zero delay shows that the value of R_0 starts increasing once the control u_1 drops after 138 days, whereas Figure 6 (a) for nonzero delay shows R_0 does not start increasing until 150 days which is slower than the zero delay case. A similar pattern can be seen in comparing the zero delay Figure 5 (b) with the nonzero delay 6 (b) where R_0 starts increasing at approximately 98 days for the zero delay case and 110 days for the nonzero case.

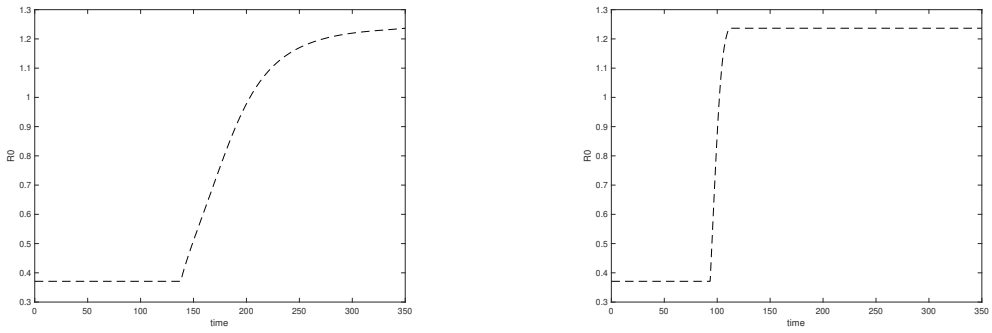

(a) (b)

Figure 5: Plots of basic reproductive number vs time for nondelay case. (a) u_1 optimal and $u_2 = 0$. (b) $u_1 = 0$ and u_2 optimal.

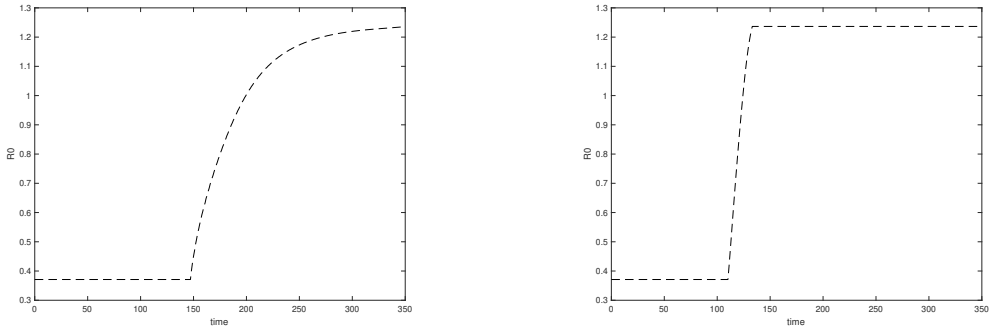

(a) (b)

Figure 6: Plots of basic reproductive number vs time for delay case ($\tau_1 = 2$ days, $\tau_2 = 4$ days). (a) u_1 optimal and $u_2 = 0$; (b) $u_1 = 0$ and u_2 optimal.

Finally, in Figure 7 we show the plots of R_0 vs u_1 and R_0 vs u_2. It can be seen that in both cases a value of approximately 0.2 gives a value of $R_0 = 1$ and could therefore be used, if required, to maintain an infection-free system.

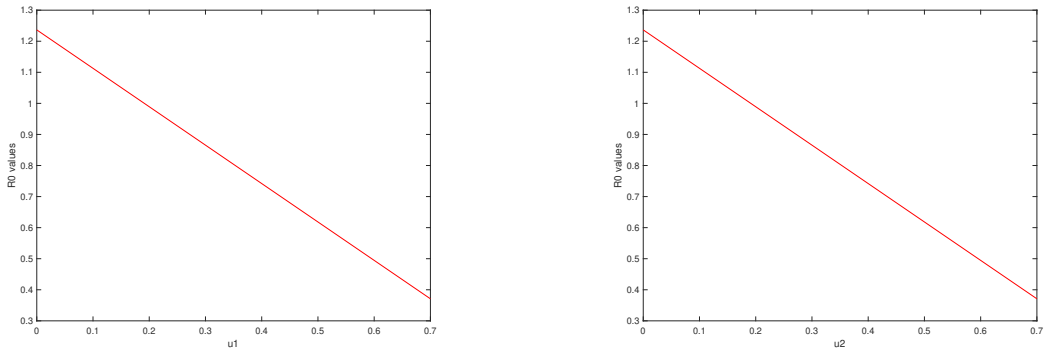

(a) (b)

Figure 7: Plots of basic reproductive number vs optimal control values for zero delay. (a) R_0 vs u_1; (b) R_0 vs u_2.

5. Conclusions

In this article, we have studied an optimal control problem for two drug therapies in a time delay model for HBV infection. The model consists of six populations: uninfected hepatocytes, infected hepatocytes, HBV DNA-containing-capsids, free viruses, antibodies and cytotoxic T-lymphocytes. The two time delays in the model are a delay in virus production after cell infection and a delay in antigenic stimulation generation. The model also includes an adaptive immune response, a cure rate for infected hepatocytes to uninfected hepatocytes and HBV DNA-containing capsids. The two optimal therapies are for blocking new infection of uninfected cells and for inhibiting viral production by infected cells. The solutions of the model are proved to be nonnegative, unique and bounded. The model is shown to have three equilibrium states, namely infection-free, immune-free and endemic. The basic reproduction number for the stability of the infection-free equilibrium has been derived and a sensitivity analysis has been carried out to determine the most important parameters to change to control the disease. The Pontryagin maximum principle is used to find the optimal control to maximize the concentrations of uninfected hepatocytes, antibodies and cytotoxic T-lynphocytes at mininmum cost. The existence of optimal control pairs is proved and an algorithm is developed for solution of the state and costate equations for the time delayed Pontryagin maximum principle. Numerical simulations are then carried out to illustrate the dynamical behavior of the solutions of the time delayed optimal control model of HBV infection. The results show that the effects of the intracellular delays is to slow down the rate of infection. Finally, the results show that the two optimal control therapies considered in this paper can reduce the basic reproductive number to less than one and can significantly reduce the concentration of infected hepatocytes, intracellular HBV DNA-containing capsids, free viruses, antibodies and cytotoxic T-lymphocytes and can also slow down the time of their epidemic peaks. Both control therapies have therefore been shown to be useful measures for reducing HBV infection. In this paper, we have shown examples of the effect of the therapy for a period of 350 days for values of parameters selected from published papers, if available, or that we assumed to be reasonable if published values could not be found.

In this paper, we have not considered the possibility of memory or history effects in the state variables of the model. There is now a large literature on fractional derivatives and integrals and their applications to develop models which include these memory or history effects. Extensive reviews of the basic concepts of fractional calculus and its applications can be found in books by Podlubny [54], Hilfer [33], Kilbas et al. [40], Petráš [53], and in the PhD thesis of Kisela [41]. In recent years, there have

also been many new definitions of fractional derivatives which have been developed for various purposes including biology. Some examples of useful fractional derivatives include Riemann-Liouville [54], Caputo [10, 54], Hadamard [39], Katugampala [35], Caputo-Fabrizio [11], Atangana-Baleanu [5, 6], and Hattaf [30, 36]. Examples of fractional calculus models related to HBV infection include Bachraoui et al. [7] and Hattaf [30, 36]. Furthermore, spatiotemporal dynamics have not been included in this study. Some works that are related to spatiotemporal dynamics include Hattaf and Yousfi [31], Hattaf [29], and Manna and Hattaf [45]. In future work, it would be interesting to develop further fractional calculus models and spatiotemporal dynamics for HBV infection models.

Acknowledgments

This work has been supported by Department of Mathematics, Faculty of Science, Naresuan University, Thailand. Pensiri Yosyingyong has been funded by DPST scholarship from the Thai government.

References

[1] R. Ahmed, D. Gray, *Immunological memory and protective immunity: understanding their relation*, Science, **272** (1996), 54–60. 1
[2] A. Alberti, S. Diana, G. Sculard, A. Eddleston, R. Williams, *Detection of a new antibody system reacting with dane particles in hepatitis B virus infection*, Br. Med. J., **2** (1978), 1056–1058. 1
[3] K. Allali, A. Meskaf, A. Tridane, *Mathematical modeling of the adaptive immune responses in the early stage of the HBV infection*, Int. J. Differ. Equ., **2018** (2018), 13 pages. 1
[4] H. Anton, C. Rorres *Elementary Linear Algebra*, Wiley, New York, 2019. 2.3
[5] A. Atangana, D. Baleanu, *New fractional derivatives with nonlocal and non-singular kernel: Theory and application to heat transfer model*, J. Therm. Sci., **20** (2016), 763–769. 5
[6] A. Atangana J. F. Gómez-Aguilar, *A new derivative with normal distribution kernel; Theory, methods and applications*, Phys. A, **476** (2017), 1–14. 5
[7] M. Bachraoui, K. Hattaf, N. Yousfi, *Qualitative analysis of a fractional model for HBV infection with capsids and adaptive immunity*, Int. J. Dyn. Syst. Differ. Equ., **12** (2022), 146–162. 5
[8] G. Birkhoff, G.-C. Rota, *Ordinary differential equations*, John Wiley & Sons, New York, (1989). 2.3
[9] V. Bruss, *Envelopment of the hepatitis B virus nucleocapsid*, Virus Res., **106** (2004), 199–209. 1
[10] M. Caputo, *Linear model of dissipation whose Q is almost frequency independent. II*, Geophys. J. Int., **13** (1967), 529–539. 5
[11] M. Caputo, M. Fabrizio, *A new definition of fractional derivative without singular kernel*, Prog. Fract. Differ. Appl., **1** (2015), 73–85. 5
[12] L. Cesari, *Existence theorems for weak and usual optimal solutions in Lagrange problems with unilateral constraints. I*, Trans. Amer. Math. Soc., **124** (1966), 369–412. 3.1
[13] F. F. Chenar, Y. Kyrychko, K. Blyuss, *Mathematical model of immune response to hepatitis B*, J. Theoret. Biol., **447** (2018), 98–110. 1
[14] F. V. Chisari, *Cytotoxic T cells and viral hepatitis*, J. Clin. Invest., **99** (1997), 1472–1477. 1
[15] S. M. Ciupe, R. M. Ribeiro, A. S. Perelson, *Antibody responses during hepatitis B viral infection*, PLoS Comput. Biol., **10** (2014), 1–16. 1
[16] J. Danane, K. Allali, *Mathematical analysis and treatment for a delayed hepatitis B viral infection model with the adaptive immune response and DNA–containing capsids*, High-throughput, **7** (2018), 35–50. 1
[17] J. Danane, A. Meskaf, K. Allali, *Optimal control of a delayed hepatitis B viral infection model with HBV DNA-containing capsids and CTL immune response*, Optimal Control Appl. Methods, **39** (2018), 1262–1272. 1, 1, 2.1
[18] R. D. Driver, *Ordinary and delay differential equations*, Springer-Verlag, New York-Heidelberg, (1977). 2.3, 2.3
[19] S. Eikenberry, S. Hews, J. D. Nagy, Y. Kuang, *The dynamics of a delay model of hepatitis B virus infection with logistic hepatocyte growth*, Math. Biosci. Eng., **6** (2009), 283–299. 1
[20] E. M. Farah, S. Amine, K. Allali, *Dynamics of a time-delayed two-strain epidemic model with general incidence rates*, Chaos Solitons Fractals, **153** (2021), 15 pages. 1
[21] W. H. Fleming, R. W. Rishel, *Deterministic and Stochastic Optimal Control*, Springer-Verlag, New York, (2012). 3.1, 3.1
[22] J. E. Forde, S. M. Ciupe, A. Cintron-Arias, S. Lenhart, *Optimal control of drug therapy in a hepatitis B model*, Appl. Sci., **6** (2016), 219–236. 1, 3.2, 3.2
[23] D. Ganem, A. M. Prince, *Hepatitis B virus infection-natural history and clinical consequences*, N. Engl. J. Med., **350** (2004), 1118–1129. 1
[24] L. Göllmann, H. Maurer, *Theory and applications of optimal control problems with multiple time-delays*, J. Ind. Manag. Optim., **10** (2014), 413–441. 3.2

[25] S. A. Gourley, Y. Kuang, J. D. Nagy, *Dynamics of a delay differential equation model of hepatitis B virus infection*, J. Biol. Dyn., **2** (2008), 140–153. 1, 1

[26] S. J. Hadziyannis, N. C. Tassopoulos, E. J. Heathcote, T.-T. Chang, G. Kitis, M. Rizzetto, P. Marcellin, S. G. Lim, Z. Goodman, M. S. Wulfsohn, Shelly Xiong, J. Fry, C. L. Brosgart, *Adefovir dipivoxil for the treatment of hepatitis B e antigen-negative chronic hepatitis B*, N. Engl. J. Med., **348** (2003), 800–807. 1

[27] S. Hagiwara, N. Nishida, M. Kudo, *Antiviral therapy for chronic hepatitis B: Combination of nucleoside analogs and interferon*, World J. Hepatol., **7** (2015), 2427–2431. 1

[28] S. Harroudi, A. Meskaf, K. Allali, *Modelling the adaptive immune response in HBV infection model with HBV DNA-containing capsids*, Differ. Equ. Dyn. Syst., **31** (2020), 371–393. 1, 2.1

[29] K. Hattaf, *Spatiotemporal dynamics of a generalized viral infection model with distributed delays and ctl immune response*, Computation, **7** (2019), 1–16. 5

[30] K. Hattaf, *On the stability and numerical scheme of fractional differential equations with application to biology*, Computation, **10** (2022), 1–12. 5

[31] K. Hattaf, N. Yousfi, *A generalized HBV model with diffusion and two delays*, Comput. Math. Appl., **69** (2015), 31–40. 5

[32] S. Hews, S. Eikenberry, J. D. Nagy, Y. Kuang, *Rich dynamics of a hepatitis B viral infection model with logistic hepatocyte growth*, J. Math. Biol., **60** (2010), 573–590. 1

[33] R. Hilfer, *Applications of Fractional Calculus in Physics*, World Scientific Publishing Co., River Edge, NJ, (2000). 5

[34] F. Ibrahim, K. Hattaf, F. A. Rihan, S. Turek, *Numerical method based on extended one-step schemes for optimal control problem with time-lags*, Int. J. Dyn. Control, **5** (2017), 1172–1186. 3.2, 3.4

[35] U. N. Katugampola, *A new approach to generalized fractional derivatives*, Bull. Math. Anal. Appl., **6** (2014), 1–15. 5

[36] K. Hattaf, *A new class of generalized fractal and fractal-fractional derivatives with non-singular kernels*, Fractal Fract., **7** (2023), 1–16. 5

[37] G. L. Kharatishvili, *Maximum principle in the theory of optimum time-delay processes*, Dokl. Akad. Nauk SSSR, **136** (1961), 39–42. 3.2

[38] M. S. Khatun, M. H. A. Biswas, *Optimal control strategies for preventing hepatitis B infection and reducing chronic liver cirrhosis incidence*, Infect. Dis. Model., **5** (2020), 91–110. 1

[39] A. A. Kilbas, *Hadamard-type fractional calculus*, J. Korean Math. Soc., **38** (2001), 1191–1204. 5

[40] A. A. Kilbas, H. M. Srivastava, J. J. Trujillo, *Theory and applications of fractional differential equations*, Elsevier, New York, (2006). 5

[41] T. Kisela, *Fractional differential equations and their applications*, (2018). 5

[42] S. Lenhart, J. T. Workman, *Optimal Control Applied to Biological Models*, Chapman & Hall/CRC, Boca Raton, FL, (2007). 3.2

[43] S. R. Lewin, R. M. Ribeiro, T. Walters, G. K. Lau, S. Bowden, S. Locarnini, A. S. Perelson, *Analysis of hepatitis B viral load decline under potent therapy: complex decay profiles observed*, Hepatology, **34** (2001), 1012–1020. 1

[44] D. G. Luenberger, *Introduction to Dynamic Systems: Theory, Models & Applications*, John Wiley & Sons, New York, (1979). 3.2

[45] K. Manna, *Dynamics of a delayed diffusive HBV infection model with capsids and CTL immune response*, Int. J. Appl. Comput. Math., **4** (2018), 16 pages. 2.1, 5

[46] K. Manna, S. P. Chakrabarty, *Chronic hepatitis B infection and HBV DNA-containing capsids: Modeling and analysis*, Commun. Nonlinear Sci. Numer. Simul., **22** (2015), 383–395. 1

[47] K. Manna, S. P. Chakrabarty, *Global stability of one and two discrete delay models for chronic hepatitis B infection with HBV DNA-containing capsids*, J. Comput. Appl. Math., **36** (2017), 525–536. 1

[48] K. Manna, K. Hattaf, *Spatiotemporal dynamics of a generalized HBV infection model with capsids and adaptive immunity*, Int. J. Appl. Comput. Math., **5** (2019), 29 pages. 2.1

[49] K. Manna, K. Hattaf, *A generalized distributed delay model for hepatitis b virus infection with two modes of transmission and adaptive immunity. A mathematical study*, Math. Methods Appl. Sci., **45** (2022), 11614–11634. 1

[50] A. Meskaf, *Optimal control of a delayed hepatitis B viral infection infection model with DNA-containing capsids, the adaptive immune response and cure rate*, Int. J. Open Probl. Comput. Sci. Math., **12** (2019), 18–33. 1, 2

[51] A. Meskaf, K. Allali, Y. Tabit, *Optimal control of a delayed hepatitis B viral infection model with cytotoxic T-lymphocyte and antibody responses*, Int. J. Dyn. Control, **5** (2017), 893–902. 1, 1, 2.1

[52] F. N. Ngoteya Y. Nkansah-Gyekye, *Sensitivity analysis of parameters in a competition model*, Appl. Comput. Math., **4** (2015), 363–368. 2.6

[53] I. Petráš, *Fractional-order Nonlinear Systems*, Springer, Heidelberg, (2011). 5

[54] I. Podlubny, *Fractional differential equations*, Academic Press, San Diego, (1999). 5

[55] L. S. Pontryagin, *The Mathematical Theory of Optimal Processes*, Routledge, (2018). 3.2

[56] Md. Samsuzzoha, M. Singh, D. Lucy, *Uncertainty and sensitivity analysis of the basic reproduction number of a vaccinated epidemic model of influenza*, Appl. Math. Model., **37** (2013), 903–915. 2.6

[57] D. Sun F. Liu, *Analysis of a new delayed HBV model with exposed state and immune response to infected cells and viruses*, BioMed Res. Int., **2017** (2017), 19 pages. 1, 2.1

[58] A. Tan, S. Koh, A. Bertoletti, *Immune response in hepatitis B virus infection*, Cold Spring Harb. Perspect. Med., (2015), 1–18. 1

[59] P. van den Driessche J. Watmough, *Reproduction numbers and sub-threshold endemic equilibria for compartmental models of disease transmission*, Math. Biosci., **180** (2002), 29–48. 2.5
[60] WHO, *Hepatitis B*, (2019). 1
[61] J. Xu, G. Huang, *Global stability and bifurcation annalysis of a virus infection model with nonlinear incidence and multiple delays*, Fractal Fract., **7** (2023), 1–35. 1
[62] P. Yosyingyong, R. Viriyapong, *Global stability and optimal control for a hepatitis B virus infection model with immune response and drug therapy*, J. Appl. Math. Comput., **60** (2019), 537–565. 1
[63] P. Yosyingyong, R. Viriyapong, *Global dynamics of multiple delays within-host model for a hepatitis b virus infection of hepatocytes with immune response and drug therapy*, Math. Biosci. Eng., **20** (2023), 7349–7386. 1
[64] N. Yousfi, K. Hattaf, A. Tridane, *Modeling the adaptive immune response in HBV infection*, J. Math. Biol., **63** (2011), 933–957. 1
[65] M.-F. Yuen, D.-S. Chen, G. M. Dusheiko, H. L. A. Janssen, D. T. Lau, S. A. Locarnini, M. G. Peters, C.-L. Lai, *Hepatitis B virus infection*, Nat. Rev. Dis. Primers, **4** (2018), 1–20. 1
[66] X. Zhou, X. Song, X. Shi, *A differential equation model of hiv infection of CD4+ T-cells with cure rate*, J. Math. Anal. Appl., **342** (2008), 1342–1355. 1
[67] K. Zhuang, *Dynamical analysis of a delayed hepatitis b virus model with immune responses*, WSEAS Trans. Math., **15** (2016), 325–334. 2.1